THE JOURNAL OF COMPARATIVE NEUROLOGY 299:421–445 (1990)

Visual Receptive Field Organization and Cortico-Cortical Connections of the Lateral Intraparietal Area (Area LIP) in the Macaque

GENE J. BLATT, RICHARD A. ANDERSEN, AND GENE R. STONER
The Salk Institute for Biological Studies, La Jolla, California 92138

ABSTRACT

The visual receptive field physiology and anatomical connections of the lateral intraparietal area (area LIP), a visuomotor area in the lateral bank of the inferior parietal lobule, were investigated in the cynomolgus monkey (*Macaca fascicularis*). Afferent input and physiological properties of area 5 neurons in the medial bank of the intraparietal sulcus (i.e., area PEa) were also determined. Area LIP is composed of two myeloarchitectonic zones: a ventral zone (LIPv), which is densely myelinated, and a lightly myelinated dorsal zone (LIPd) adjacent to visual area 7a. Previous single-unit recording studies in our laboratory have characterized visuomotor properties of area LIP neurons, including many neurons with powerful saccade-related activity. In the first part of the present study, single-unit recordings were used to map visual receptive fields from neurons in the two myeloarchitectonic zones of LIP. Receptive field size and eccentricity were compared to those in adjacent area 7a. The second part of the study investigated the cortico-cortical connections of area LIP neurons using tritiated amino acid injections and fluorescent retrograde tracers placed directly into different rostrocaudal and dorsoventral parts of area LIP. The approach to area LIP was through somatosensory area 5, which eliminated the possibility of diffusion of tracers into area 7a.

Unlike many area 7a receptive fields, which are large and bilateral, area LIP receptive fields were much smaller and exclusively confined to the contralateral visual field. In area LIP, an orderly progression in visual receptive fields was evident as the recording electrode moved tangentially to the cortical surface and through the depths of area LIP. The overall visual receptive field organization, however, yielded only a rough topography with some duplications in receptive field representation within a given rostrocaudal or dorsoventral part of LIP. The central visual field representation was generally located more dorsally and the peripheral visual field more ventrally within the sulcus. The lower visual field was represented more anteriorly and the upper visual field more posteriorly. In LIP, receptive field size increased with eccentricity but with much variability within the sample.

Area LIPv was found to have reciprocal cortico-cortical connections with many extrastriate visual areas, including the parieto-occipital visual area PO; areas V3, V3A, and V4; the middle temporal area (MT); the middle superior temporal area (MST); dorsal prelunate area (DP); and area TEO (the occipital division of the intratemporal cortex). Area LIPv is also connected to area TF in the lateral posterior parahippocampal gyrus. Although area LIPd has many of the same cortico-cortical connections as LIPv, some differences were apparent. Area LIPd and not LIPv has connections with visual areas TEa and TEm (anterior and medial divisions of the intratemporal cortex) and with multimodal area IPa (subdivision of association cortex in caudal bank of superior temporal cortex) in the superior temporal sulcus. A topographic relationship between rostrocaudal parts of area LIP (including both LIPv and LIPd) and the lateromedial

Accepted July 5, 1990.

Richard A. Andersen is now at the Department of Brain and Cognitive Science, Massachusetts Institute of Technology, 77 Massachusetts Avenue, Cambridge, MA 02139. Address reprint requests there.

Gene J. Blatt is now at the Department of Anatomy and Neurobiology, Boston University School of Medicine, 80 East Concord Street, Boston, MA 02118.

parts of prefrontal cortex across areas 8a (frontal eye fields) and the medial portion of area 46 was also apparent. Intrinsic connections of LIP with other areas in the inferior parietal lobule included a feedforward projection to area 7a and connections with the bimodal ventral intraparietal area (VIP) as well as with somatosensory area 7b (PF). Some retrogradely labeled cells were seen in area 5, but this projection was not confirmed by control injections placed in the medial bank of the intraparietal sulcus (area PEa). An interesting observation was that the input into areas PEa and LIP from parieto-occipital visual areas (medial dorsal parietal area [MDP] and area PO) was found to be topographically organized such that MDP and the dorsal part of PO project to area PEa, while ventral PO and a few MDP neurons project to the opposite bank in LIP. This "visual" input to area PEa was also seen in single-unit recordings in area 5 in which a small number of visually responsive cells were identified (i.e., 7 of 204 neurons). All remaining neurons mapped in area 5 were highly responsive to joint position, movement, and/or touch.

These anatomical and physiological data demonstrate that area LIP is a unique visual area in posterior parietal cortex, with histological, anatomical, and physiological properties different from other areas in the inferior parietal lobule. Analysis of feedforward and feedback projections suggests that area LIP occupies a high position in the overall hierarchy of extrastriate visual processing areas in the macaque brain.

Key words: inferior parietal lobule, single-unit-recording, visual receptive fields, associational connections, autoradiography, fluorescent retrograde tracers, area PEa, area 7a

It is becoming increasingly evident that the macaque inferior parietal lobule is a heterogenous structure composed of a number of cortical fields. In this report, we examined an area in the lateral bank of the intraparietal sulcus, the lateral intraparietal area (area LIP). Area LIP was originally described by Andersen et al. ('85b) on the basis of its relatively stronger projection to area 8a of Walker ('40) in the frontal lobe compared to surrounding posterior parietal areas. Area LIP comprises approximately the caudal half of area POa of Seltzer and Pandya ('80) and Pandya and Seltzer ('82). On the basis of cytoarchitecture, Seltzer and Pandya ('80) have divided area POa into two subdivisions, POae (external) and POai (internal). Also, two very different myeloarchitectural patterns emerge within LIP: a dorsal lightly myelinated zone (LIPd) and a ventral heavy myelinated zone (LIPv; Siegel et al., '85). Area LIP is separated from area 7a (a portion of the original 7a of Vogt and Vogt, '19) or PG (von Bonin and Bailey, '47; see Andersen, '87) dorsally and from the ventral intraparietal area (area VIP; Maunsell and Van Essen, '83; Colby et al., '89; Duhamel et al., '89) ventrally. Physiological studies have recently found that area LIP contains an abundance of neurons that are highly responsive to saccadic eye movements (Siegel et al., '85; Gnadt et al., '86; Andersen et al., '87; Gnadt and Andersen, '88; Barash et al., '89) and neurons with visual receptive fields (Gnadt et al., '86). Of

Abbreviations

ai	arcuate sulcus, inferior ramus
as	arcuate sulcus, superior ramus
ce	central sulcus
Ci	cingulate sulcus
Cl	claustrum
deg	degrees
DP	dorsal prelunate area
DY	diamidino yellow retrograde tracer
FB	fast blue retrograde tracer
fo	fronto-orbital sulcus
gl	glia
Id	dysgranular Insula
io	Inferior occipital sulcus
ip	Intraparietal sulcus
IPa	subdivision of association cortex in the caudal bank of superior temporal cortex
l	lunate sulcus
la	lateral fissure (Sylvian fissure)
LP	lateral posterior thalamic nucleus
LIP	lateral intraparietal area or POa in the lateral bank of ip
MDP	medial dorsal parietal area
MST	middle superior temporal area
MT	middle temporal area
p	principal sulcus
pc	postcentral sulcus
PE	area 5 in the superior parietal lobule
PEa	sulcal part of area 5
PGm	medial area PG
PO	parieto-occipital visual area
pos	parieto-occipital sulcus
prCe	precentral gyrus
prce	precentral sulcus
Prt.a	anterior pretectal nucleus
Pul.l	lateral pulvinar
RF	receptive field
SII	secondary somatosensory area
SC	superior colliculus
sts	superior temporal sulcus
TEa, TEm, TEO	anterior, medial, and occipital divisions of infratemporal cortex
TF	lateral posterior parahippocampal gyrus
tmp	posterior middle temporal sulcus
VIP	ventral intraparietal area
V1, V2, V3, V3A, V4	visual areas 1, 2, 3, 3A, and 4
1, 2, 3a, 3b	primary somatosensory cortex
4	primary motor cortex
5	area PE on the medial bank of ip
6	premotor area
7a	area PG on the convexity of the inferior parietal lobule
7b	area PF of posterior parietal cortex
8a	frontal eye fields
24a	ventral part of anterior cingulate cortex
45, 46	parts of prefrontal cortex

141 cells taken from 76 penetrations in awake behaving monkeys, Gnadt et al. ('86) classified 42% of LIP neurons as light sensitive, 23% as saccade-related, 7% as saccade-related and light sensitive, and 17% as intended movement cells. The intended movement cells had sustained activity above background during the time period for which the monkey was required to remember the target position but withhold eye movement (Gnadt and Andersen, '88). Half of the saccade-related neurons of area LIP have presaccadic activity. Unlike area LIP, fewer neurons in area 7a were saccade-related and most of these cells had post-saccadic responses (Gnadt and Andersen, '88; Andersen et al., '90a; Andersen and Gnadt, '89). At the anterior and caudal borders of area LIP, area VIP of Maunsell and Van Essen ('83) has strong connections with the middle temporal area (MT) and contains both visual and somatosensory neurons (Colby et al., '89; Duhamel et al., '89).

Although the connections of area 7a in nonhuman primates have been extensively demonstrated (Mesulam et al., '77; Seltzer and Van Hoesen, '79; Hedreen and Yin, '81; Pandya and Seltzer, '82; Seltzer and Pandya, '84; Andersen et al., '85b; Asanuma et al., '85; Siegel et al., '85; Yeterian and Pandya, '85; Andersen, '87; Neal et al., '88a,b; Andersen et al., '90a), a systematic anatomical study of area LIP has been lacking. Thus, in the present study, the connections of LIP with visual, limbic, unimodal, and multimodal association cortices in the macaque brain were investigated. Some data have been reported previously regarding area LIP connections. Area LIP has much stronger connections with frontal eye field area 8a than does area 7a (Barbas and Mesulam, '81; Siegel et al., '85; Andersen et al., '90a). Asanuma et al. ('85) have reported differences in the subcortical connections of the two areas. Area 7a has connections with the medial pulvinar whereas area LIP is connected to the lateral pulvinar (Asanuma et al., '85). In addition, area LIP sends a projection to the intermediate and deep layers of the superior colliculus (Asanuma et al., '85; Colby and Olson, '85; Lynch et al., '85) while no such projection has been reported for area 7a (Lynch et al., '85).

In the present investigation, we were also interested in determining how the visual receptive fields of the light-sensitive LIP neurons are organized. To accomplish this, visual receptive fields were accurately mapped in lightly anesthetized monkeys using an eye ring to stabilize the eye and prevent drift (Allman and Kaas, '71). Each microelectrode track was subsequently reconstructed and the size and organization of the receptive fields within area LIP were determined. Injections of both anterograde and retrograde tracers were made directly in area LIP or in area PEa on the medial bank of the intraparietal sulcus (control injections) using an approach so as to avoid area 7a. Area LIP was found to be almost entirely connected to other visual cortical areas and the cells almost exclusively responded to visual stimuli; however, a projection from somatosensory area 7b was found. In contrast, single-unit recordings in area 5 (including area PEa) in the superior parietal lobule confirmed the somatosensory properties reported for area 5 neurons in previous studies (Duffy and Burchfield, '71; Sakata et al., '73; Mountcastle et al., '75; MacKay et al., '78; Hyvarinen, '82; Seal et al., '82, '83) but also revealed the presence of a small number of neurons with visual responses (Hyvarinen, '82). Earlier reports of the present investigation have been presented in abstract form (Blatt et al., '87; Stoner et al., '87a,b).

MATERIALS AND METHODS

Visual receptive field mapping and subsequent anatomical tracing studies were performed in five adult cynomolgus monkeys (*Macaca fascicularis;* cases M-100, M-107, M-108, M-109, and M-110). In each animal, single unit recording was performed in one hemisphere for 6–12 weeks. Subsequent to the physiological mapping study, three monkeys received a single injection of tritiated amino acids and two injections of retrogradely transported fluorescent dyes into area LIP. In each of the other two animals, two tracer injections were placed in area LIP (one anterograde and one retrograde tracer), while one injection was placed into sulcal area 5 (area PEa) in the opposite bank of the intraparietal sulcus (one retrograde tracer injection). Thus from the five cases, a total of five amino acid injections and 8 fluorescent dye injections were made into different rostrocaudal and dorsoventral parts of area LIP and 2 fluorescent dye injections were made in area 5.

Surgical procedures

A single surgical procedure with full aseptic precautions was performed for each monkey. All instruments, accessories, and gowns were sterilized in an autoclave. The primate was administered intravenous 5% dextrose in 0.9% sterile sodium chloride. Surgical anaesthesia was induced with an injection (IM) of ketamine hydrochloride (Ketalar) and was maintained with intravenous sodium pentobarbital (Nembutal, 35 mg/kg) in 0.9% sterile saline. The animal was given an IM injection of 0.1 ml atropine (0.4 mg/ml) for vasodilation and 0.2 ml of dexamethasone (4 mg/ml; 1.5 ml added to the sodium chloride IV bag prior to surgery and 0.5 ml given IM) as an anti-inflammatory agent. The monkey was placed in a stereotaxic apparatus and warmed with a heating pad. The skull was shaved and wiped with Betadine and a midline incision was made dorsally with skin and underlying muscle reflected laterally. A series of 6–8 small screws and one longer ground screw were placed into the skull. A trephine was used to make a craniotomy over the posterior parietal cortex, which was located by stereotaxic coordinates. A stainless steel recording chamber (Narishige) was mounted over the craniotomy and secured with additional small screws. A metal T-bar (used for holding the head still while recording) was placed rostrally at a 90° angle to the cranial surface. The dorsal portion of the skull was then covered with layers of dental acrylic (mixture of dental powder and self curing acrylic) which further held the recording chamber and T-bar in place. The wound around the acrylic covering was sutured with 4-0 black silk suture (Ethicon) and topical triple antibiotic ointment (Goldline) was applied. Finally, on the day of surgery and for a period of 3 days following surgery, each animal was administered an IM injection of 500 mg of ampicillin sodium (Wyeth omnipen-N) as a prophylactic measure.

Animal preparation and single-unit recording procedures

Following placement of a recording chamber over the posterior parietal cortex and a 4 day recovery period, single unit recordings were made every 3–4 days using a Narishige microdrive micromanipulator in an X-Y coordinate frame. The recording chamber was placed over the superior parietal lobule on a 15° rostrocaudal angle. This approach resulted in electrode penetrations which traversed area 5, a somatosensory area, across the intraparietal sulcus and

then into area LIP. Therefore, electrode penetrations did not pass through area 7a, a visual area immediately adjacent to area LIP. However, some additional penetrations were made directly into areas 7a and VIP to compare visual receptive fields and define the borders of LIP. Penetrations were made using glass coated platinum-irridium wire electrodes which were advanced at 1 μm intervals by the digital pulse microdrive (Narishige) through the silicon oil (dimethylpolysiloxane) filled chamber. Each electrode was made by hand: mounted into a holder, placed in a BAK metal electrode etcher to make appropriate tip profiles, viewed under the microscope, placed in a micromanipulator, glassed (Corning glass), and subsequently tested for the proper range of impedance (1.0–2.5 MΩ). The electrode signal was fed into a BAK preamplifier with Krone-Hite bandpass filter, BAK window descriminator and a Tektronix analogue oscilloscope. The recording chamber was cleaned daily with 0.9% sterile saline, and a few drops of gentamycin sulfate (Garamycin), and Maxitrol suspension were applied to the dural surface and sides of the chamber. When needed, the excess connective tissue was scraped off the dural surface with aseptic periosteal elevators.

Prior to each recording session (every 3–4 days) the monkey was lightly anaesthetized with Ketalar (supplemental doses approximately every half hour) and given an initial injection of 0.1 ml (1 mg) triflupromazine hydrochloride (Vesprin), which acts as a muscle relaxant to offset the increased muscle tone from the ketamine. The monkey sat in a primate chair with his head fixed (T-bar attached to a head holder). To stabilize one eye for receptive field mapping, an eye ring preparation (Allman and Kaas, '71) was applied. The eye was first anaesthetized with 0.5% dibucaine and dialated with 1% cyclopentolate hydrochloride (Cyclogel). A stainless steel eye ring with a recessed inner surface (inside diameter = 11 mm; outside diameter = 13 mm) was held against the sclera with light pressure or with one drop of Histoacryl adhesive applied to the inner surface of the eye ring. The eye ring contained two cusps which held back the upper and lower eye lids. A metal arm, connected to the edge of the ring, attached to a ball joint and was locked into position off to one side away from the animal's head. To keep the surface of the eye moist, a gas permeable contact lens (diameter = approximately 10.5 mm; base curve = 6.25; planar; Syntex Ophthalmics, Inc. or Contact Lens, Inc.) with a wetting solution (Wet N' Soak, Allergan) was applied. Additional lubrication of the eye was achieved by often applying a few drops of wetting solution manually or under computer control.

A coaxial halogen ophthalmoscope (Welch-Allyn) was used to map the fovea onto a tangent screen. The ophthalmoscope was attached to a snake clamp locked to a C-clamp on the primate chair. After visualizing the fovea, the head of the ophthalmoscope was reversed 180° and projected onto the tangent screen placed 57 cm from the monkey. A hand-held halogen streak retinoscope provided the visual stimulus which was a bar of light that could be rotated 360° to provide varying orientation. For each electrode penetration, the edges of the receptive fields were mapped onto large white drawing paper taped to the tangent screen. Visual receptive field maps were obtained for neurons in area LIP, and for purposes of comparison, additional maps were obtained for some area 7a neurons. In most instances the background lighting was 1 cd/m^2. Since the receptive field maps were made on the tangent screen in two dimensional coordinates, receptive field calculations were adjusted for tangent error. Each receptive field map was placed on a large transparent plexiglass plate with the corrected coordinates drawn on it to determine the final coordinates. Receptive field size for each LIP unit was calculated by computing the square root of the area. The relationship between receptive field size and eccentricity among the entire sample of units was then tested with a significance of regression test and analysis of variance (Sokal and Rohlf, '73).

During the last 2 weeks of recording, marking lesions (4 μA at 4 seconds) were made for subsequent reconstruction of electrode penetrations. Generally, two marking lesions were made in a given penetration: one just ventral to a portion of area LIP in the white matter, and one in area 5, dorsomedial to area LIP. Also, at the time of sacrifice, four guide wires, positioned in microdrive coordinates, were lowered through the recording chamber into the brain. These provided reliable reference points for subsequent reconstruction of the microelectrode placement.

Injections of anatomical tracers

Subsequent to the receptive field mapping of area LIP neurons, injections of neuroanatomical tracers were made into area LIP under physiological control. This was achieved via a custom attachment to the Narishige microdrive, which allows the placement of a lengthened Hamilton syringe down a guide tube following single unit recording at the same site. In each monkey, a single injection of a mixture of 0.2 μl (approximately 20 μCi) of L-[4,5-^{3}H]-leucine (specific activity = 60.0 Ci/mmol, New England Nuclear) and L-[2,3-^{3}H]-proline (specific activity = 27.2 Ci/mmol; New England Nuclear) concentrated to 100 μCi/μl of 0.9% sterile saline was made into area LIP via the anteroposterior approach through area 5. Each injection was performed over a 10 minute period and an additional 10 minutes was allowed before withdrawal of the syringe to prevent leakage of the radioisotope up the needle track. In each animal, two additional injections were made into different rostrocaudal regions of area LIP using the fluorescent retrogradely transported dyes fast blue (FB), which labels the cytoplasm of the soma blue (Kuypers et al., '80), and diamidino yellow (DY), which labels the nucleus yellow (Keizer et al., '83) [dyes obtained from Dr. Illing, Gross-Umstadt, Germany]. Each injection consisted of 0.2 μl of a 5% aqueous solution of FB or 0.2 μl of a 3% solution of DY using a 1 μl modified Hamilton syringe.

Histological procedures

A postoperative survival time of 7–10 days for the amino acids and 10–14 days for the fluorescent dyes was used. Each animal was deeply anaesthetized with an overdose of sodium pentobarbitol and transcardially perfused with 250 ml of 0.9% sterile saline followed by 2 liters of 4% paraformaldehyde (both at room temperature) and then with an additional 2 liters of cold 5% glycerin in 4% paraformaldehyde. Blocking of the brain was performed by precise maneuvering of a large scalpel blade with the animal in a stereotaxic apparatus. Following removal of the brain, the blocks were placed in 15% glycerol in 4% paraformaldehyde overnight, followed by 20% glycerol in 4% paraformaldehyde for 2–3 days. Each block was frozen in crushed dry ice and cut into 30 μm coronal sections on a sliding microtome. Five sections were mounted from every ten. The first two

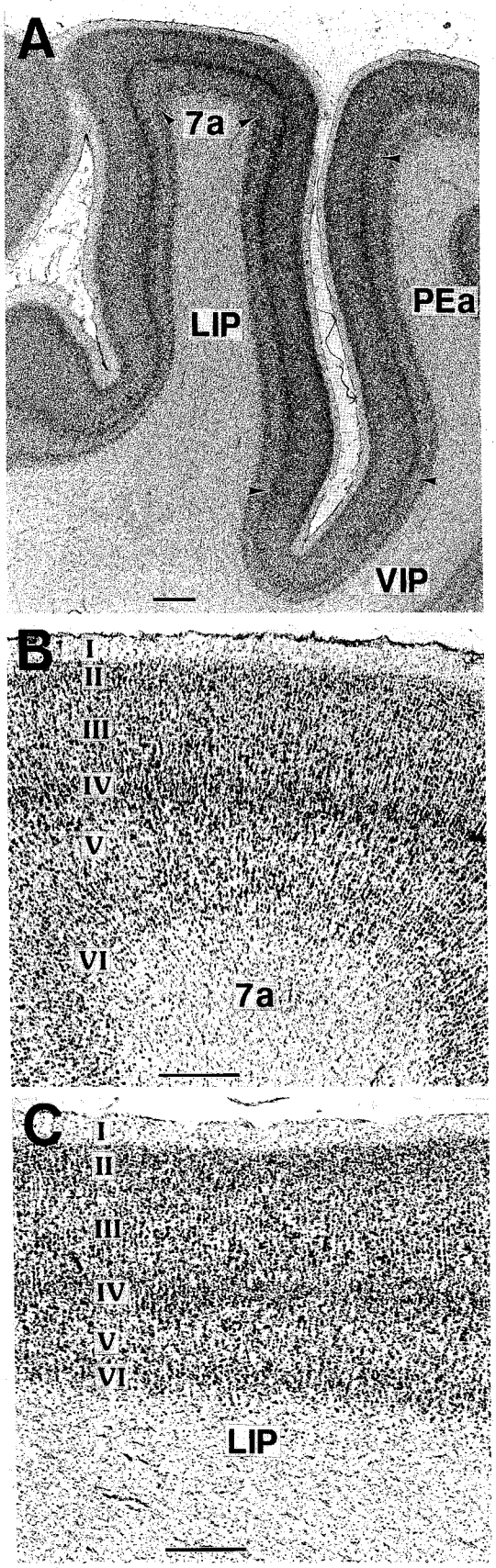

series were immediately mounted on gelatin subbed slides for fluorescence and kept in the cold room (one series was later thionin stained to examine cytoarchitecture), the third and fourth series were processed according to the method of autoradiography (Cowan et al., '72) and later lightly counterstained with thionin, and the fifth series was stained for myelin from the modified protocol of Gallyas ('79). For the autoradiographic series, the slides were defatted and dipped under safelight conditions in NTB2 nuclear emulsion (Kodak; 1:1 dilution with distilled water) and allowed to dry for three hours, boxed and refrigerated (at 4 degrees C). The exposure time for the two series was 8 and 10 weeks. Slides were developed in D-19 at 15°C for 4 minutes followed by 30 seconds in distilled water and 6 minutes in Kodak Rapidfix. The slides were scraped on the reverse side with a single-edged razor blade, thionin stained, and mounted with Permount. The anterograde label from the autoradiographic series was drawn by hand from a Zeiss microscope. Each fluorescence series was charted on an X-Y plotter coupled to a mechanical microscope stage equipped with epifluorescence, and stored on an Apple IIe computer.

RESULTS

Parcellation of architectonic cortical fields

In agreement with previous studies, examination of coronal sections stained for Nissl substance (Seltzer and Pandya, '80) or myelin (Siegel et al., '85) have revealed distinct differences in the cyto- and myeloarchitecture of area LIP and area 7a (Figs. 1, 2). In thionin stained sections, layers II through VI in area 7a cortex yield a columnar appearance with the thin cell columns oriented orthogonal to the lobular surface (Fig. 1A,B). While in area 7a the pyramidal cells in layers IIIc and Va are organized in vertical arrays (Fig. 1B), the cells in these layers in area LIP are scattered and disorganized (Fig. 1C). While some of these features may be attributable to the location of these fields on the convexity of the lobule (7a) or in the sulcus (LIP), there are additional cytoarchitectonic differences in the two areas. For example, granular layer II is more densely packed in area LIP and the layer II-III border is very distinct. In contrast, the layer II-III border is less distinct in area 7a and layer IV is denser in area 7a than in LIP (compare Fig. 1B and C). Pyramidal neurons in layers III and V are very distinct in both LIP and 7a (Fig. 1C) but the layers V-VI border is more highly differentiated in LIP than in 7a (Fig. 1B,C). With regard to myeloarchitecture, one part of area LIP is a thickly myelinated region in the lateral bank (arrowheads in Fig. 2A–D) that extends through

Fig. 1. **A:** Thionin-stained coronal section through the intraparietal sulcus including area 7a at the convexity of the inferior parietal lobule (ip), area LIP along the lateral bank of ip, area VIP at the fundus and area PEa (sulcal part of area 5) on the medial bank of ip in the superior parietal lobule. **B:** Enlarged view of a Nissl stained coronal section through area 7a. Note the columnar arrangement of the cell layers. Layer IV is particularly distinct, while layers V and VI are not clearly separated. In **C,** an enlarged view of the lamina in area LIP, a thick layer II is evident, a less distinct layer IV but clearly segregated layers V and VI. The pyramidal cells are not aligned in a columnar fashion as in B but are more scattered and are deeply stained. At the ventral border of LIP is area VIP, the ventral intraparietal area (A), which has a thin layer IV. On the medial bank, layer IV becomes closely packed in area PEa neurons (see A). Scale bar in A = 1.0 mm; in B,C = 0.5 mm.

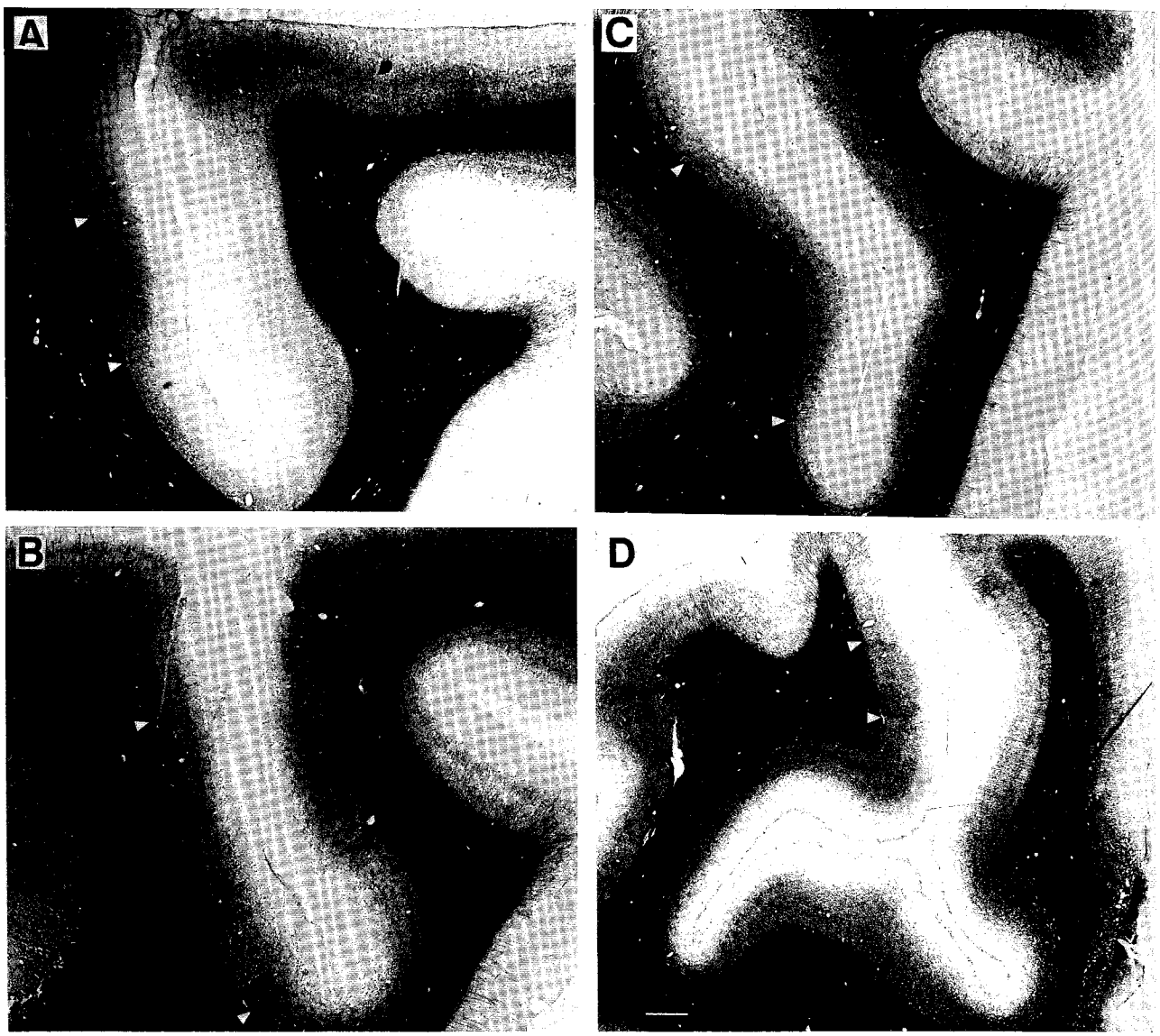

Fig. 2. **A–D:** Myelin stained coronal sections through different rostrocaudal levels through the intraparietal sulcus. In the most rostral section (A) the ventral part of area LIP (LIPv) contains an abundance of myelin stained fibers (white arrowheads), whereas the adjacent region dorsal to the heavy myelinated zone (LIPd) has less dense staining. This difference in staining intensity becomes more apparent in sections B–D. Note that the intensity of staining also decreases in area VIP, the area adjacent and ventral to the heavily myelinated zone (see area below lower arrowhead in sections A–C. Also note the difference in the angle of the intraparietal sulcus and the surrounding cortex as the sections are viewed in a progressively caudal manner. In rostral sections A and B, the intraparietal sulcus points medially (i.e., to the right) then changes its orientation in a ventral turn as seen in C. With the presence of the anectant gyrus caudally in section D, the fundus of the intraparietal sulcus opened up to include "buried cortex." At this caudalmost level, area LIP is very narrow. In two of the five cases, LIP ended at a slightly more rostral level to that shown in this case (M-100) in section D. Scale bar in D = 1.0 mm.

many rostrocaudal sections but dorsally the upper portion of the lateral bank is lightly myelinated (e.g., dorsal to the upper arrowhead in Fig. 2B–D). The thickness of the myelin increases again at the convexity of the inferior parietal lobule in area 7a (Fig. 2B; refer to Fig. 1A for location). Ventral to the myelinated part of LIP is another area of reduced myelination, area VIP (Figs. 1A, 2A–C), which extends rostro-caudally along the ventralmost aspect of the lateral bank, the fundus, and the ventral part of the medial bank of the intraparietal sulcus (also refer to Fig. 7). Proceeding up the medial bank, a densely myelinated area that is part of area 5 (area PEa; Fig. 2B,C) emerges adjacent to VIP.

Visual receptive fields of LIP neurons

In the five cases from 86 microelectrode penetrations, 228 light sensitive neurons in area LIP were identified in anesthetized macaques. With the eye ring preparation to stabilize the eye, visual receptive field maps were constructed for 104 neurons in area LIP and an additional 22 fields were mapped for area 7a and area VIP neurons. A comparison of receptive field size of representative neurons

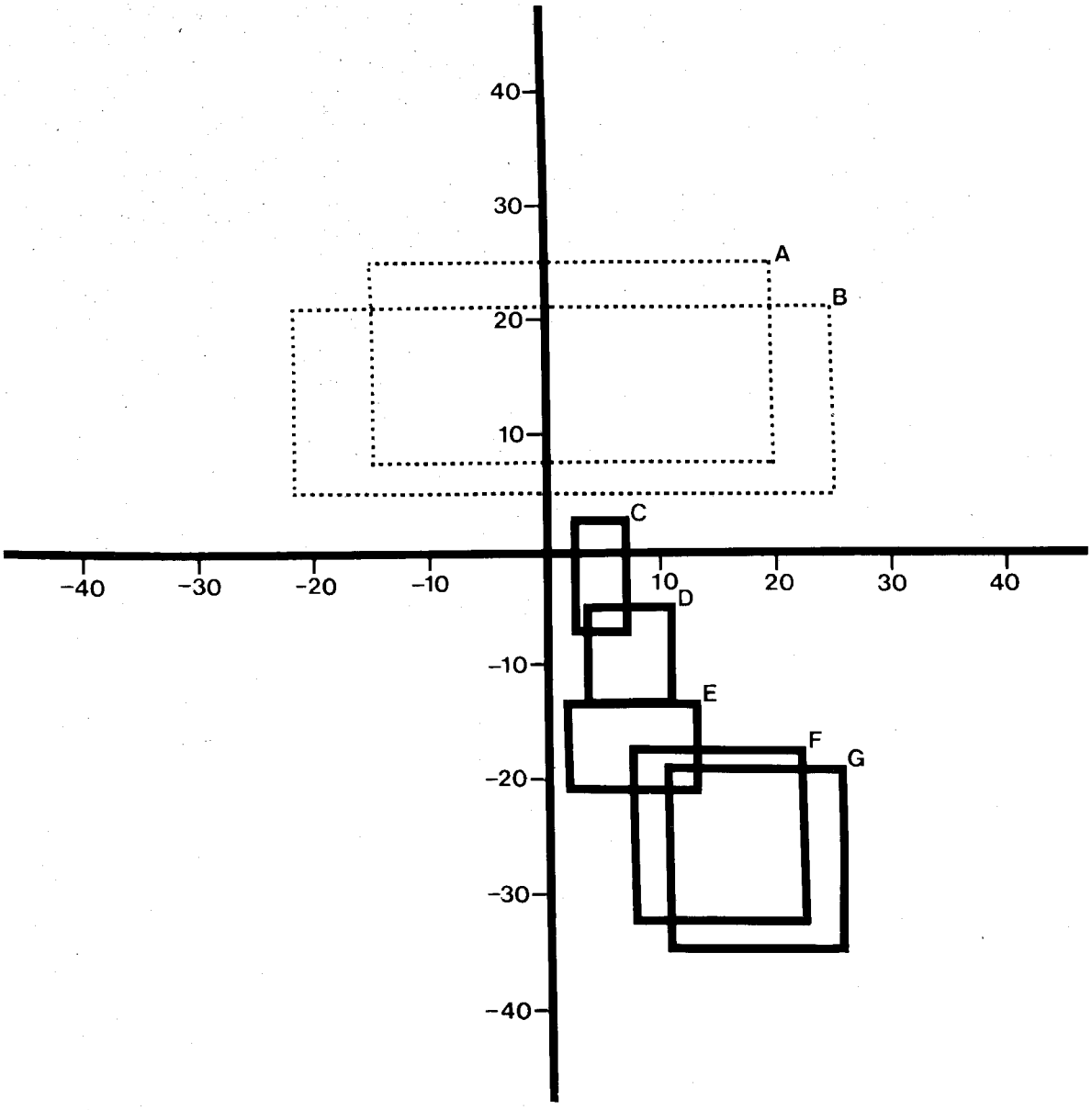

Fig. 3. Line drawing illustrating the difference in size and location of visual receptive fields in areas 7a and LIP. The origin on the graph (0,0) represents the mapped coordinate for the fovea in this case (M-107). As seen in A and B, area 7a neurons had characteristically large bilateral receptive fields. In contrast, area LIP neurons had smaller receptive fields (C–G) that were restricted to the side that was opposite the stimulated retina (i.e., contralateral). Note the local progression of receptive fields toward the lower field and the corresponding increase in field size from this penetration in LIP (C–G).

in area LIP and area 7a from case M-107 is illustrated in Figure 3. The fovea is represented at the origin on the graph. As seen in Figure 3A,B from case M-108, visual receptive fields for area 7a neurons are typically very large and bilateral (e.g., covering approximately 15° to 25° bilaterally). In contrast, area LIP neurons are smaller in size (Fig. 3C–G) and vary from about 5° × 5° near the foveal representation (Fig. 3C) to about 15 × 15° toward the periphery (Fig. 3F–G). Unlike many area 7a neurons, most LIP receptive fields are contralateral to the stimulated retina. The microelectrode penetration in Figure 3C–G was typical of a penetration that proceeded on an angle down the lateral bank. An orderly progression in receptive fields was evident such that the receptive field of each subsequent neuron either slightly overlapped or bordered on the proceeding neurons' receptive field. In another example (case M-110), seen in Figure 4, the electrode tracks were reconstructed from marking lesions and pins (see Methods) and were on a 15° anteroposterior angle through the microelectrode recording chamber traversing area 5 en route to area LIP (upper drawings). The two microelectrode penetrations were made at the same anteroposterior level and were spaced 1 mm apart. The receptive field centers from 14 mapped area LIP neurons and 6 mapped area VIP neurons from two microelectrode penetrations (penetration #16, cells 10–19; and penetration #30, cells 51–60) are illus-

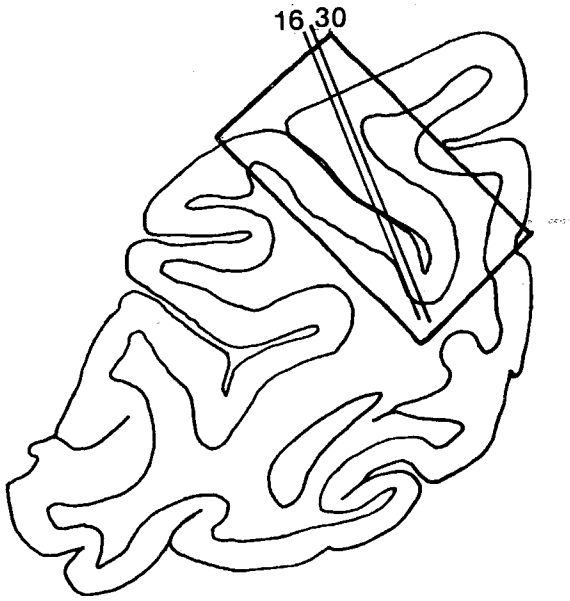

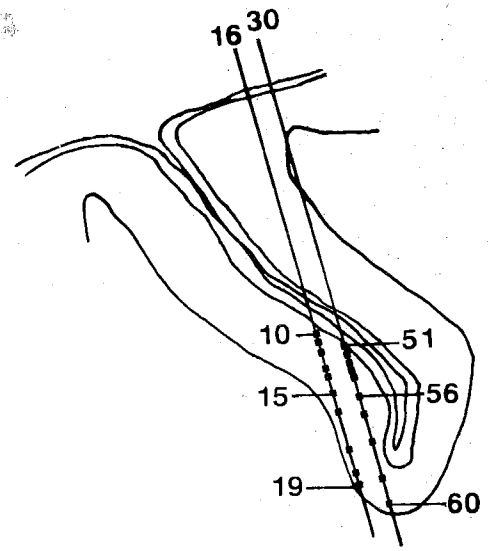

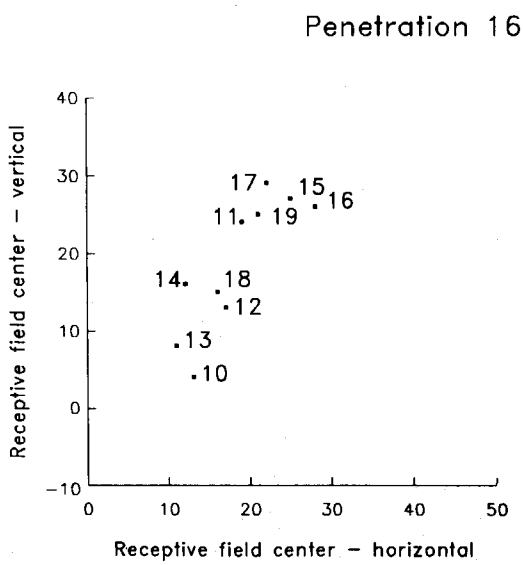

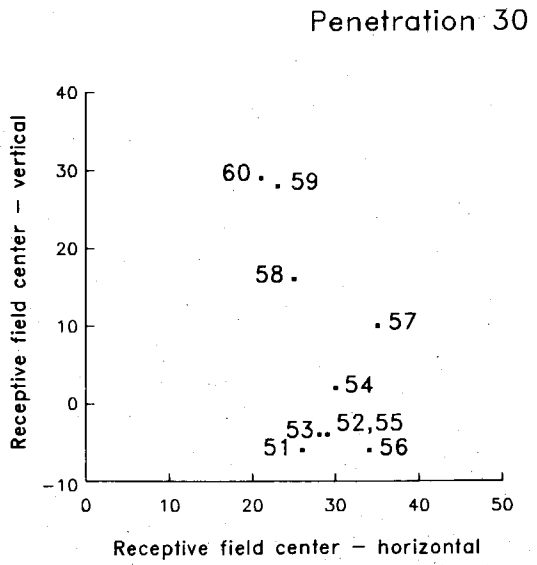

Fig. 4. Line drawings illustrating two microelectrode penetrations (#16 and #30) which were made at a similar anteroposterior level spaced 1 mm apart, in areas LIPv and VIP. The upper two drawings illustrate the angle of approach and the mapped cells (cell #10–19 in penetration #16 and cells #51–60 in penetration #30) and their locations. The lower drawings illustrate the receptive field centers for the 20 neurons in the two penetrations. From myelin-stained sections from this case, it was subsequently determined that units #10–16 and #51–57 were in area LIPv and units #17–19 and #58–60 were in area VIP. A shift in receptive field centers from upper to middle fields and from central to more peripheral fields was evident as the electrode moved medially (i.e., to the right). Note however, that the drawings are two-dimensional reconstructions of a representative coronal section through area LIP whereas the actual microelectrode penetration was at an angle to the lateral bank and traversed many rostrocaudal sections. At the bottom of the bank in VIP, however, another shift to the upper field was seen (e.g., receptive field centers for cells #18, 19 and #57–60).

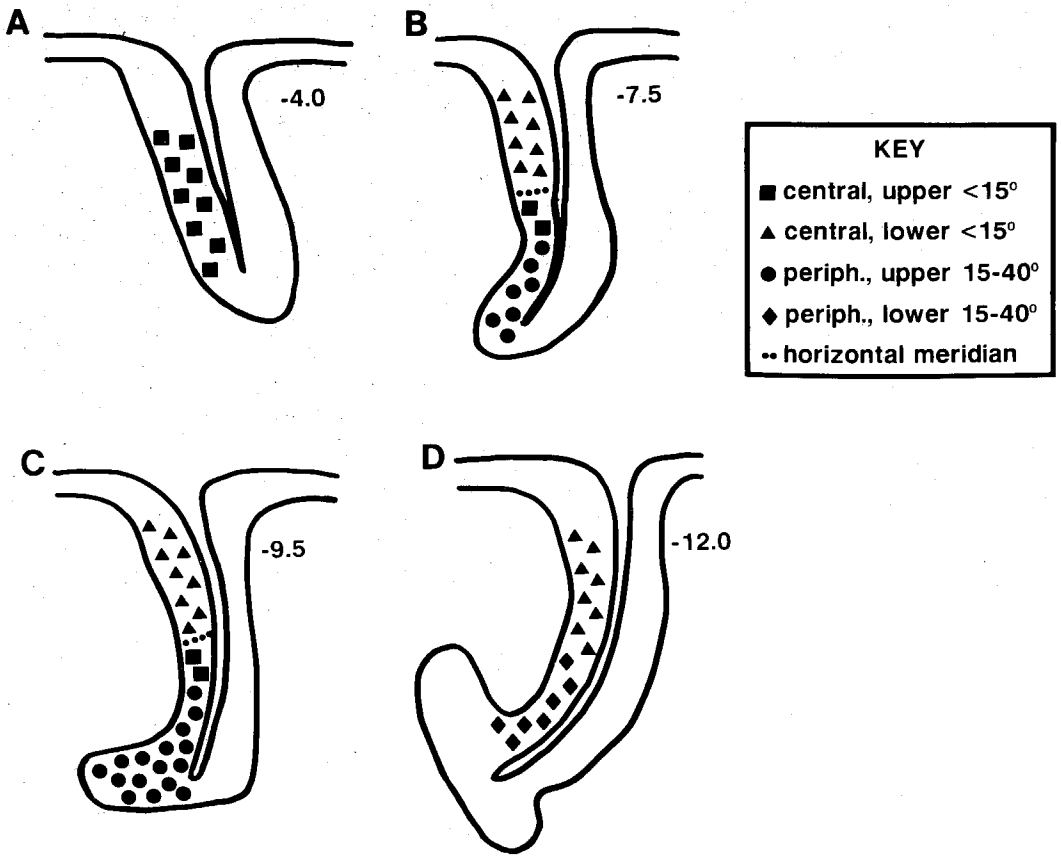

Fig. 5. Summary diagram of visual receptive field organization of 104 mapped neurons in area LIP. The negative numbers to the right of each figure indicate approximate distance from stereotactic zero. At the most rostral level (**A**), the receptive fields were mostly found in the upper visual field within 15° of the vertical meridian. In **B**, the upper field representation shifted more to the periphery and was found in cells mapped in LIPv. The horizontal meridian (dotted line) is crossed about halfway down the bank with lower field representation in LIPd. A similar situation is seen in **C** but at the caudalmost levels, lower field representation predominates (**D**) with more peripheral fields found in the depths of the lateral bank.

trated in the lower drawings. In this case, the myelinated part of area LIP extended far down the lateral bank of the intraparietal sulcus and included units #10–16 and units #51–57, whereas the units recorded in the bottom of the lateral bank (units #17–19 and #58–60) were determined by myeloarchitecture to lie in the lateral part of area VIP. In penetration #16, the LIP units' receptive field centers (units #10–16) were scattered in the upper quadrant but were located mostly between 15°–25°) of eccentricity. In contrast, the LIP units' receptive field centers (units #51–57) in penetration #30 were clustered around the border between the upper and lower quadrants and shifted out to 25–35° of eccentricity. In contrast, the receptive field centers (units #17–19 and #58–60) of VIP neurons were clustered in similar locations on the map at 15°–25° of eccentricity in the upper visual quadrant. Among the numerous microelectrode penetrations in area LIP in the five cases, there were many examples of overlap in the visual representation of the contralateral hemifield. For example, some units had a location 3–4 millimeters from others within area LIP but having virtually the same visual representation as well as similar receptive field size.

The overall distribution of visual receptive fields in area LIP is illustrated in a composite drawing in Figure 5. The negative numbers to the right of each figure represent the approximate distance in millimeters from the anteroposterior stereotactic "0." In the most rostral (i.e., anterior) part of area LIP the mapped contralateral visual receptive fields were localized to the upper quadrant within 15° of the foveal representation (Fig. 5A). Proceeding caudally through LIP (Fig. 5B), the dorsal part of LIP contained many cells with representations within 15° of the fovea but shifting in representation to the lower visual field. In contrast, the ventral part of LIP contained neurons with more peripheral receptive fields with upper field representation (Fig. 5B,C). At this level, the horizontal meridian was identified as approximately halfway down the lateral bank (Fig. 5B,C). The receptive field progressions (mainly from lower to upper field representation) were consistent, progressing from the lightly myelinated (LIPd) part and through the densely myelinated part (LIPv) of LIP. It is also interesting that this trend continued to the very bottom of the lateral bank into area VIP except at the most caudal level. Thus the ventral border between LIP and VIP at the fundus of the intraparietal sulcus was difficult to determine physiologically. The most caudal part of area LIPv, as illustrated in Figure 5D, contained peripheral receptive fields in the lower contralateral quadrant (representing a downward shift from the more rostral parts of LIPv), while neurons in caudal LIPd contained more central receptive fields in the lower quadrant (similar to the representation of more rostral LIPd units). This caudal part of LIP becomes

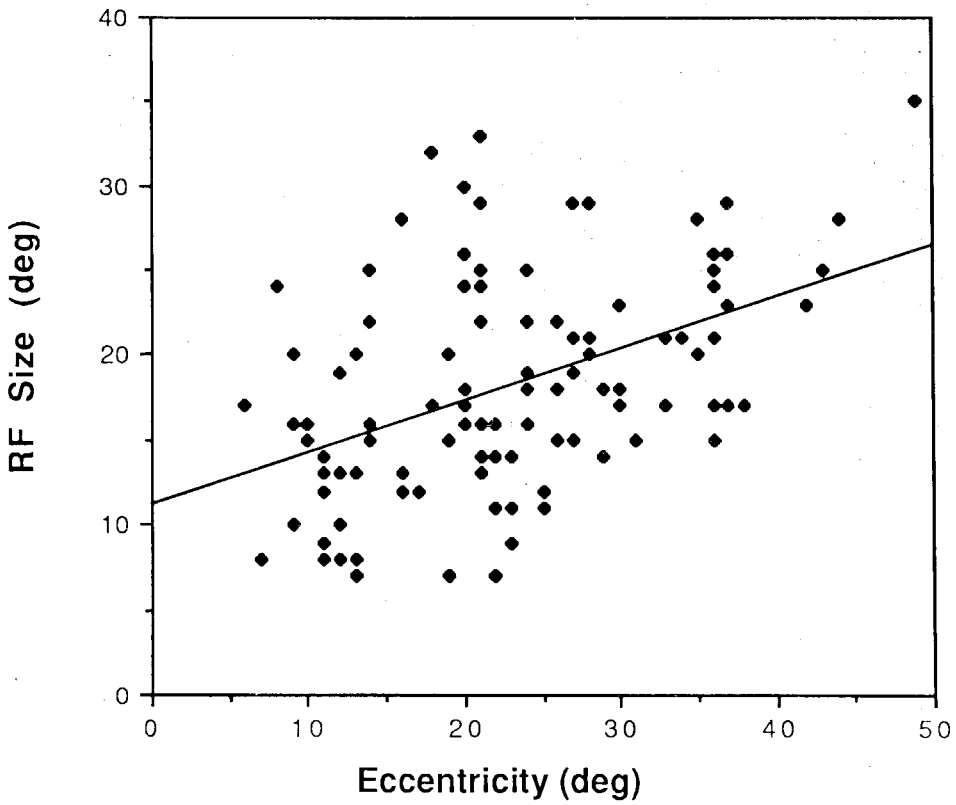

Fig. 6. Graph illustrating receptive field (RF) size (i.e., square root of the area) plotted against RF eccentricity. A regression line of best fit is indicated from the raw values plotted for 104 mapped RFs. The y intercept is just above 11 degrees and progresses to about 24° at 40° of eccentricity at an angle of about 0.3 (i.e., 30°). Although much variability is seen by widely scattered points, a rough progression to slightly larger fields with increasing eccentricity is evident. See text for further description.

limited to a smaller portion of the lateral bank as it approaches the anectant gyrus (refer to Fig. 2D). Therefore, from the sample of mapped neurons in the present study, upper field representation was concentrated in the rostral two-thirds of LIP, while lower field representation was restricted to the caudal two-thirds of LIP. Central representations of the visual field were located more dorsally, and peripheral representations were located more ventrally in LIP.

A linear regression graph of receptive field size and eccentricity is shown in Figure 6. The data include all recording sites for 104 LIP neurons in the five cases. The mean receptive field size increased from about 14° at 10° of eccentricity to about 23° at 40° of eccentricity (Fig. 6). The plotted line through the graph represents the best-fitting line from a least squares regression. The formula $y = a + bx$ where "y" is the least squares regression line and is equal to "a" (11.199), which is the y-intercept plus "b" (0.30431), the slope of the line. The "r squared" value was 0.21, indicating that 21% of the variability in receptive field size is a function of receptive field eccentricity (Sokal and Rohlf, '73). The variability in receptive field size at a particular eccentricity was usually not seen in a given penetration through area LIP but was very apparent when different penetrations were compared. The greatest variability in receptive field size for LIP neurons occurred between 15° and 25° of eccentricity with receptive field sizes ranging from about 7.5° to 33°, although there were more units sampled (n = 37) within this range of eccentricity than any of the other panels. The tests of significance (see Materials and Methods) yielded a P value < 0.05, indicating that this variability in receptive field size in relation to eccentricity was significant.

Anterograde tracing studies in LIP

A single injection of tritiated amino acids was made into area LIP in each of five monkeys. We will describe the results from two of these cases (M-110 and M-108), as one other case (M-107) yielded similar results and another two cases (M-100 and M-109) hit only a part of LIP and spread into two adjacent areas yielding mixed results. A photomicrograph of the injection site from case M-110 in rostral area LIPv is shown in Figure 7. The approach to area LIP through area 5 is clearly visible by the presence of glia in the upper medial bank of the intraparietal sulcus (small arrow) and from electrode tracks (wide arrows) in the lateral bank. This injection site includes all cell layers in the ventral part of area LIP. As seen in a schematic diagram illustrating the same autoradiographic case (i.e., case M-110) the injection site extends through many rostrocaudal sections (shaded regions in Fig. 8, sections 3–4). The drawing in the upper left illustrates the lateral surface of the macaque brain and the levels (1–5) at which the coronal sections in Figure 8 were drawn. Labeled fibers are seen leaving the area of the injection site ascending dorsally toward area LIPd and area

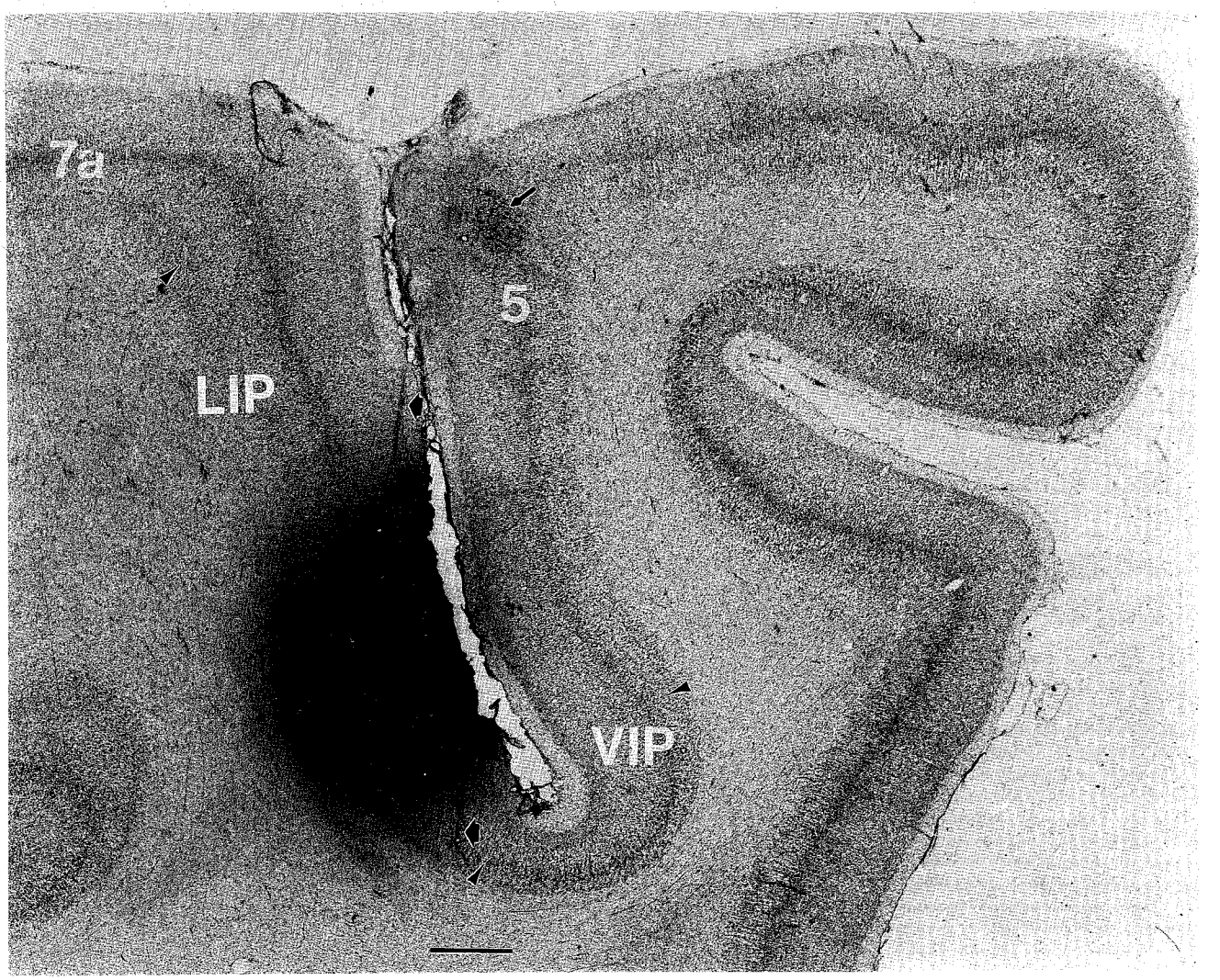

Fig. 7. Photomicrograph of a Nissl stained coronal section showing a tritiated amino acid injection site in the rostral part of LIPv in case M-110. Note the glia (small arrow) in area 5 and the microelectrode tracks (wide arrows) which indicate the approach to LIP via the superior parietal lobule instead of through area 7a which could confound results. The arrowheads delineate the borders of LIPv and VIP. Scale bar = 1.0 mm.

7a (section 3). In the same coronal section, fibers also course ventrally to supply area VIP on the medial bank. The small amount of isotope observed in area 5 in sections 3 and 4 was probably due to some spreading along the syringe path through the medial bank (see Fig. 7). Additional fibers course rostrally to the prefrontal cortex supplying frontal eye field area 8a and prefrontal cortex area 46 (section 1). Fibers also course laterally around the floor of the rostral superior temporal sulcus (STS) to terminate in areas MT and MST (sections 3–4). An example of a feedback projection from LIP to MT in this case is shown in Figure 9. As seen under darkfield illumination (Fig. 9A), some anterograde label in layer I in area MT was seen. This small amount of anterograde labelling was restricted to layer I and not seen in any of the other layers such as layer VI, also typical of a feedback projection. In contrast, the anterograde label in MST was across all cell layers as seen in the darkfield photomicrograph in Figure 10A. This pattern of anterograde label represents a strong "intermediate" type of cortical projection from LIP. In Figure 8, some of the fibers course around STS to continue caudally and laterally to supply ventral area V4 (layers I and II in Fig. 8, section 3; layers I and VI in section 4) and layers II through V in the lateral posterior parahippocampal gyrus (area TF) and in infratemporal visual area TEO (section 2). Still other fibers course posteriorly from the injection site to supply layers I through III in area V3A in the anectant gyrus (Fig. 8, section 5). In a few sections, additional fibers were seen to terminate in posterior visual area PO (not illustrated). Some fibers take a caudal course to terminate in subcortical areas such as the lateral pulvinar (Pul.l) and anterior pretectal nuclei (Prt.a) in section 2 and superior colliculus (SC). In section 3, area V3A was labeled in superficial layers only (layers I through 3; Fig. 8, section 5).

A schematic drawing of a second autoradiography case (M-108) is illustrated in Figure 11. The injection site in M-108 was dorsal and caudal to that in case M-110, in the mid-upper portion of the lateral bank of the intraparietal sulcus (sections 3–4). This injection was centered in LIPv but also included the ventral part of LIPd. In this case, a

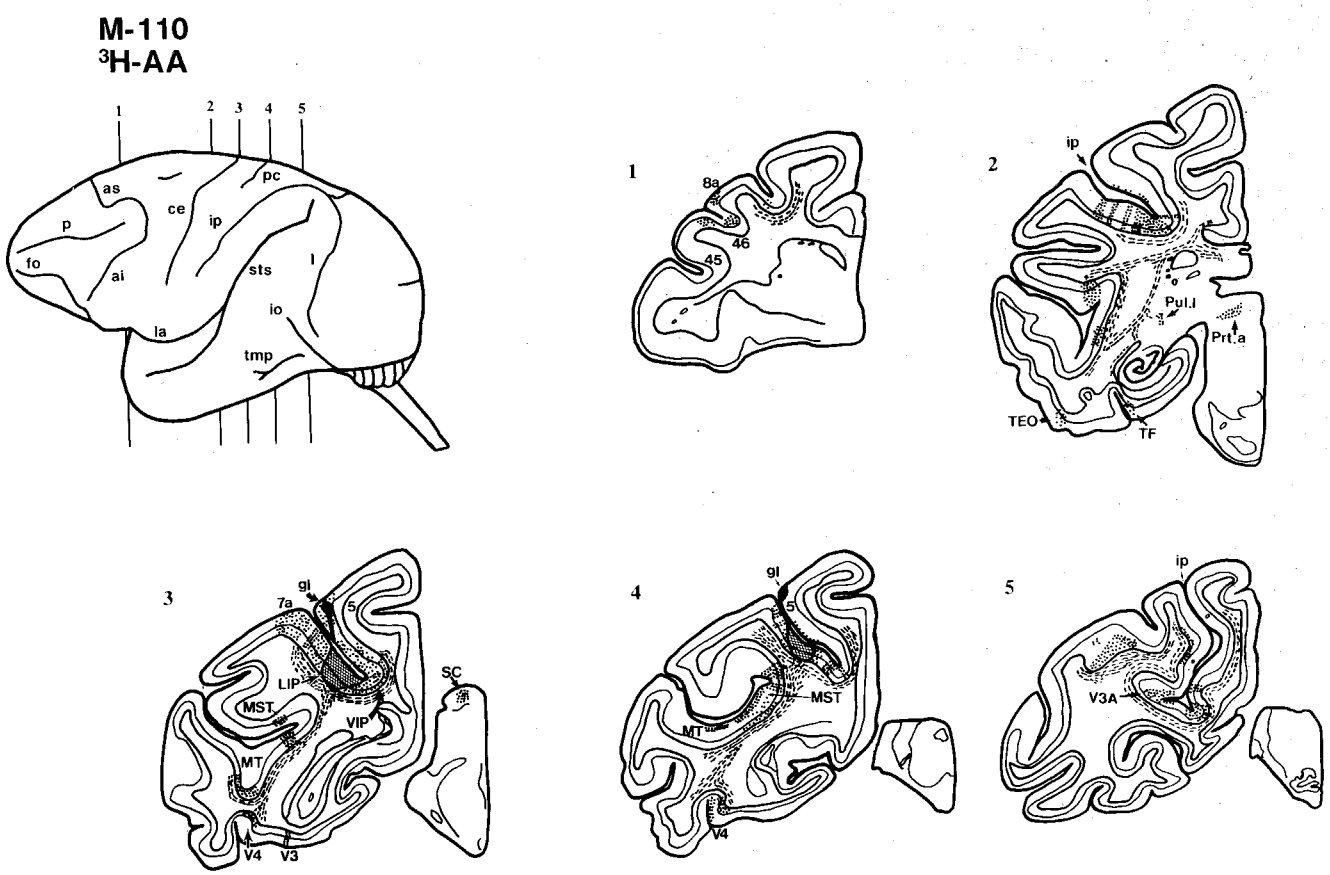

Fig. 8. Line drawings illustrating the injection site and pattern of anterograde labeling in case M-110 from a tritiated amino acid injection in rostral-intermediate LIP. The drawing at the upper left shows the lateral surface of the macaque brain and the sulci and shows the level from which sections 1–5 were taken. The injection site, shown in sections 3 and 4 (also seen in Fig. 7) is limited to LIPv in section 3 but it extends caudally into the dorsal part of LIPv (section 4). In section 1, fibers project into prefrontal cortex with anterograde label seen in areas 8a and 46. In section 2, fibers project within the intraparietal sulcus (ip) and terminate in a bandlike fashion across all cell layers. Some fibers project to the temporal lobe labeling medial TF, area TEO, and areas MT and MST, which is also seen in sections 3 and 4. Subcortical projection zones include the lateral pulvinar (Pul.l) and anterior pretectal nucleus (Prt.a) in section 2 and the superior colliculus (SC) in section 3. Also in section 3, anterograde label is seen in VIP and in ventral areas V3 and V4. The V4 label continues caudally in section 4 and anterograde label is also present in area V3A in section 5. Caudal to section 5, additional anterograde label was present in areas PO, DP and dorsal V3 (not illustrated). See text and Figures 9 and 10 for laminar pattern of anterograde labeling in this case.

very small quantity of radioisotope diffused into area 5 along the needle track. Fiber patterns in the white matter were quite similar in the two cases, but there were some differences in anterograde label in cortical areas. For example, anterograde label was seen in the inferotemporal cortex in case M-108 labeling layers I through IV in areas TEm, TEa, and IPa (section 2) and layers I, III, IV, and V in ventral V4 (section 3). Similar to case M-110, feedforward projections were found to layer IV in area 7a in section 3 (also see Fig. 12) and to layers III, IV, and V in frontal eye field area 8a, areas 46 (section 1), and area TF (section 2). Anterograde label was seen in layers I and VI (i.e., feedback) in area MT again, giving the appearance of a "weak" projection (section 3). Similar to case M-110, an intermediate type labeling was seen across most cell layers in MST in case M-108 (sections 3 and 4). Anterograde label was also seen in area V3A (section 5), in layer I in the dorsal prelunate area (DP; section 5) and in area VIP (section 4). Anterograde labeling was also seen in layers I, II, and III and some in layer V in visual area PO and in the superficial layers in dorsal area MDP (section 5). Subcortical projections in case M-108 were seen to the superior colliculus, anterior pretectal nucleus, lateral pulvinar and, in the claustrum (Cl) and putamen (Put; section 2).

Fluorescent retrograde tracing studies in LIP

In the four cases illustrated (M-108, M-110, M-107, M-100), five fluorescent dye injections were made into different rostrocaudal levels of area LIP. From the most rostral injection (case M-108; Fig. 13), the FB injection site (section 2) extended approximately 5 mm down the lateral bank and was largely restricted to LIPv. A few retrogradely labeled cells were found in frontal eye field area 8a but more labeled cells were seen in prefrontal area 46 (section 1). Fast blue labeled cells were also seen in areas 7a (sections 2–4), 7b (section 3), MT and MST (sections 3–4), TF (not illustrated), in the posterior portion of visual area PO (section 5), and in the anectant gyrus in area V3A (section 5). A sparse projection was also seen from area PGm (section 4).

Case M-110 illustrates the results from dye injections into an intermediate (FB) and a more caudal (DY) level of

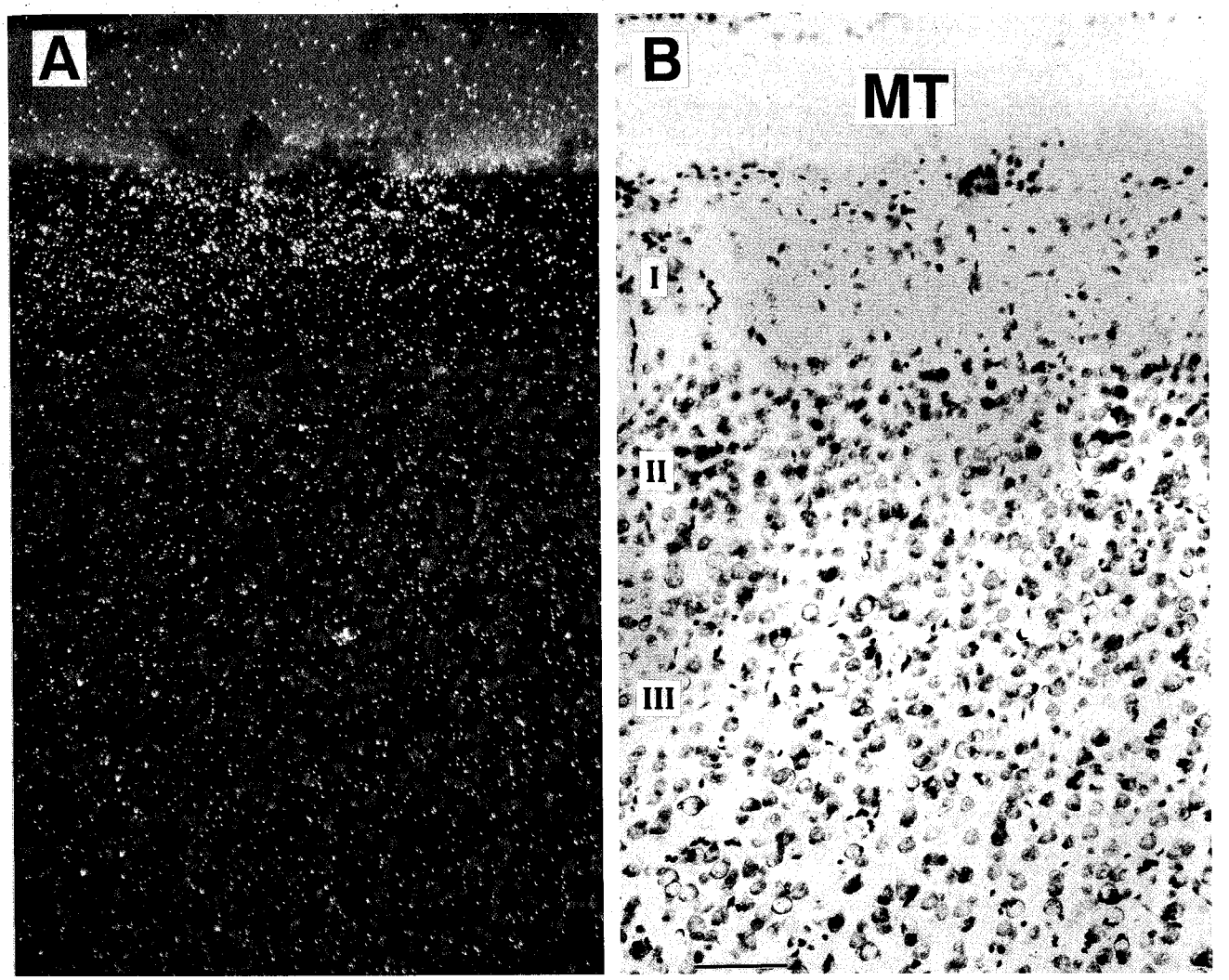

Fig. 9. Example of a "feedback" projection to area MT from a tritiated amino acid injection into area LIP in case M-110 shown in Figures 7 and 8. As shown in the darkfield photomicrograph in **A,** the "weak" anterograde label was restricted to layer I in MT. The corresponding thionin stain of the same coronal section is presented in **B.** Scale bar in B = 50 μm.

area LIPv (Fig. 14). In the intermediate injection, FB labeled cells were abundant in the lateral part of frontal eye field area 8 (triangles in section 1), in areas V3 (section 4), V3A (section 5), and V4 (sections 3–4), in the anteromedial portion of area PO (section 2) and in area MST (sections 3–4). A more sparse projection is seen from area MT (section 3). Many FB labeled cells were seen in LIPd (sections 2 and 4), but fewer labeled cells were found in area 7a. The DY injection in case M-110 (dots in Fig. 14) in a more caudal part of LIPv largely resulted in retrogradely labeled cells in similar areas as reported for case M-108. In contrast to the labeled cells in the lateral part of area 8a from the FB injection of this case (M-110), many DY labeled cells were restricted to the medial part of 8a (section 1). In the DY injection, labeled cells were also seen in area PGm (section 2 and 3), in areas PO (section 5), MT (section 3), MST (sections 3 and 4), at the area 7a/7b border (section 3), VIP (sections 2–4), and in areas V3 (sections 4 and 5) and V4 (sections 3–5).

In case M-107, a DY injection was made in the most posterior portion of LIPv at the rostral part of the anectant gyrus (Fig. 15). Labeled cells were found in similar brain areas such as areas MT, MST, TF, V3A, V4, 7a, and in LIPd, VIP, and PO. However, one noteworthy difference was that in area 8a, labeled cells were only found in the most medial cortical field, near the border of area 6 (section 1).

Thus, a comparison of all four injections from the three cases described above (i.e., M-108, M-110, and M-107) and from two reciprocal anterograde cases (M-108 and M-110) demonstrates a lateromedial topography of labeled regions in the prefrontal cortex (including area 8a and the medial part of area 46) from corresponding dye injections in the rostrocaudal sectors within LIP. In addition, there is consistent retrograde and anterograde labeling in many extrastriate visual areas such as V3, V3A, V4, MT, MST, 7a, VIP, and PO. Thus the connections of all these areas to LIP are reciprocal. The most rostral LIP injections resulted in labeled cells or terminals in somatosensory area 7b. Since

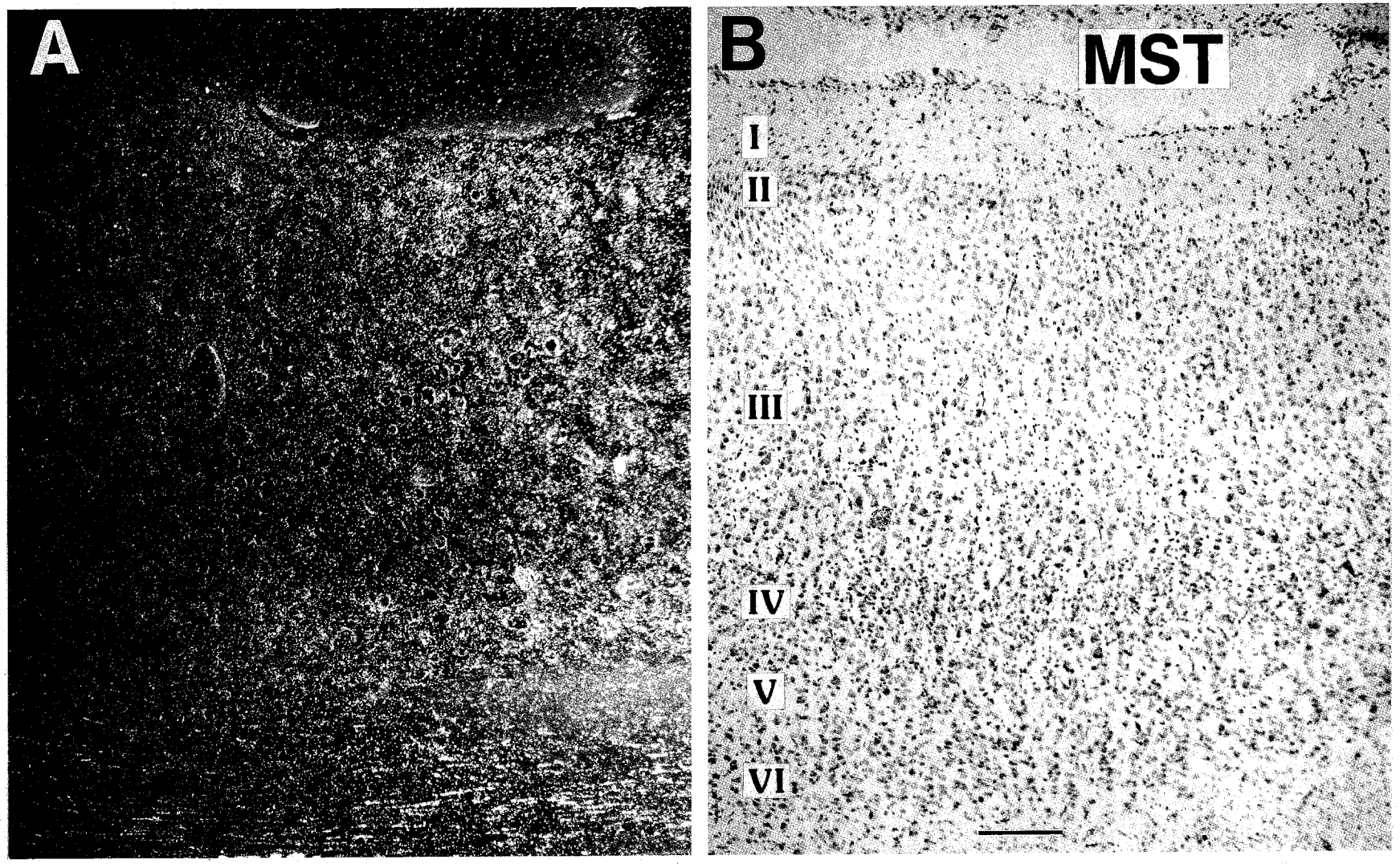

Fig. 10. Example of an "intermediate" projection to area MST from a tritiated amino acid injection into area LIP in case M-110. As shown in the darkfield photomicrograph in **A,** anterograde label was present throughout all cell layers in MST and not restricted to particular lamina as was the situation in Figure 9. Scale bar in **B** = 200 μm.

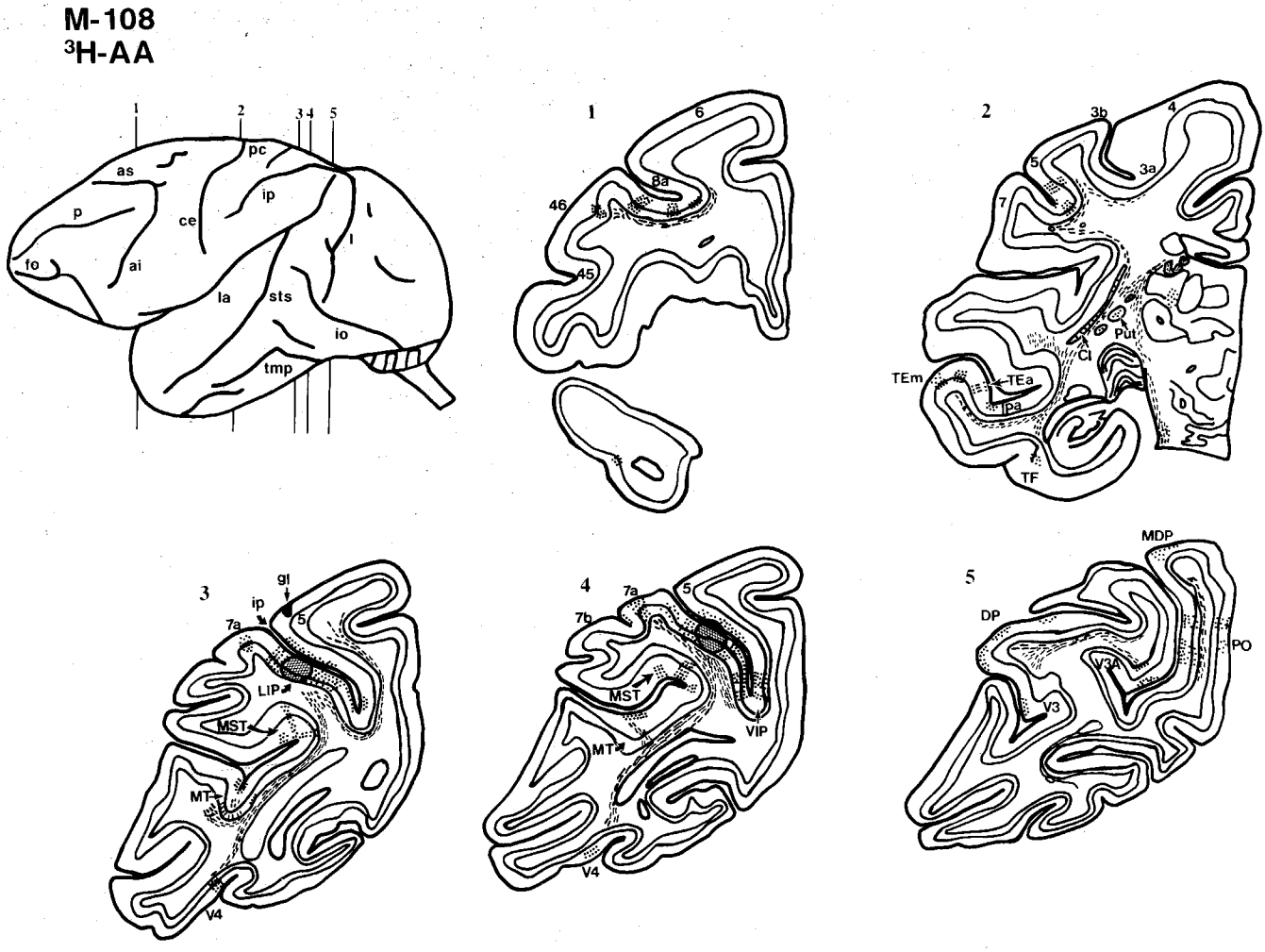

Fig. 11. Line drawings illustrating the injection site and pattern of anterograde labeling in case M-108 from a tritiated amino injection in intermediate-caudal levels of LIP. As seen in sections 3 and 4, the injection site is found at the border of LIPv and LIPd, including parts of both sectors (refer to Fig. 2). In section 1, anterograde label was seen in area 8a in the lateral bank of the superior arcuate sulcus (as) as well as some label in area 46. In section 2, anterograde label was seen in the parietal lobe in areas 5 and 7 and in the temporal lobe in areas TF, TEa, TEm, and multimodal area IPa (see Pandya and Yeterian, '85; Baylis et al., '87). Additional areas of anterograde label in section 2 include the claustrum (Cl) and putamen (Put). In section 3 at the level of the injection site, anterograde label was seen in areas MT, MST, V4, and 7a. The label in area 7a was mainly restricted to layer IV (see Fig. 12). The anterograde label in section 4 was very similar to section 3 but more extensive label was seen in area VIP. Caudally in section 5, an extensive projection was seen to area PO and a light projection to area MDP dorsal V3 and dorsal prelunate area (DP).

the approach to area LIP was through area 5, some leakage of tracer along the needle path may account for the small amount of label in that area.

Since all the injections described above were largely restricted to LIPv, two additional fluorescent dye injections were made in LIPd. An example of such a case (M-100) is illustrated in Figure 16. This FB injection was centered in the lightly myelinated part of area LIP at an intermediate rostrocaudal level (Fig. 16). It is noteworthy that retrograde labeling of cells from this case was largely similar to the results from injections in LIPv in the previous three cases with retrogradely labeled cells in areas PO, V3, V3A, 7a, 7b, 46, MST, and VIP. However, no labeled cells were seen in area MT, indicating that the light MT projection zone to area LIP was restricted to LIPv. This result confirms Ungerleider and Desimone's ('86b) observation that injections of anterograde tracers in area MT labelled only the densely myelinated part of the lateral bank. Unlike all previous retrograde cases in the present study, labeled cells were seen in the dysgranular insula (Id) and in area 24 in the anterior cingulate gyrus, which is more typical of projections to area 7a (Siegel et al., '85; Andersen et al., '89). Also, very few labeled cells were seen in area 8a, while many cells were localized in a cluster in area 46, this is also typical of projections to area 7a.

Single-unit recordings in area 5

In contrast to the single-unit recordings in LIP that revealed virtually all visual cells with only a few somatosensory cells, recordings in area 5 yielded the opposite results. As shown in Table 1, of 204 cells in area 5, 197 cells vigorously responded to mechanical stimulation (i.e., flexion, extension, or rotation) at one or more joints (usually in the

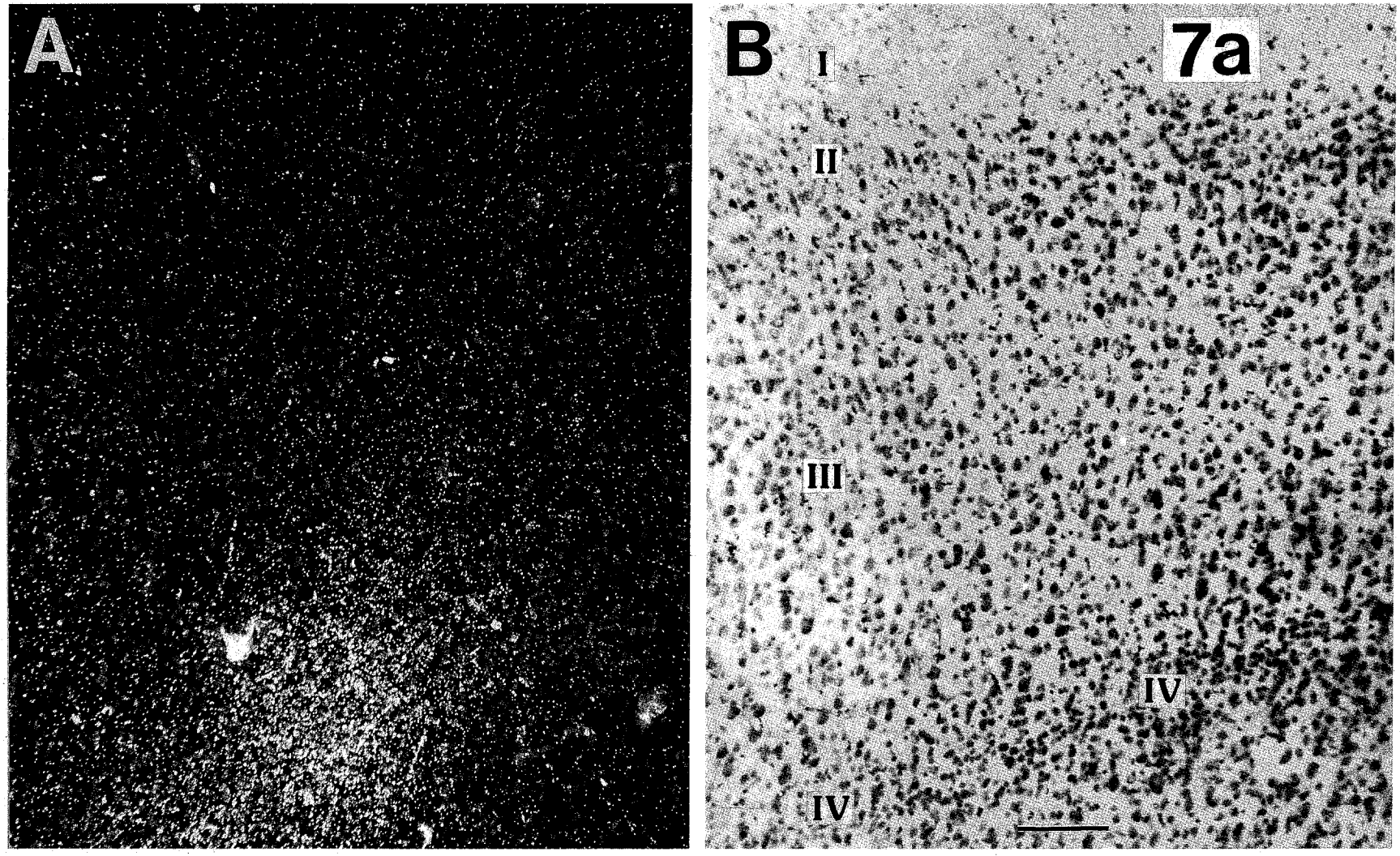

Fig. 12. Example of a "feedforward" projection to area 7a from a tritiated amino acid injection in case M-108 into area LIP. In the darkfield photomicrograph in **A,** anterograde label is largely restricted to the lower part of layer III and to layer IV (see Nissl stained section in **B**). Compare this pattern of termination with Figures 9 and 10 that demonstrate feedback and intermediate patterns. From these patterns of anterograde label, a hierarchy of visual connections to and from visual areas in the inferior parietal lobule and other projection zones in frontal, temporal, parietal and occipital areas in the macaque brain was constructed (see Figs. 26, 27 in Andersen et al., '89). Scale bar in B = 100 μm.

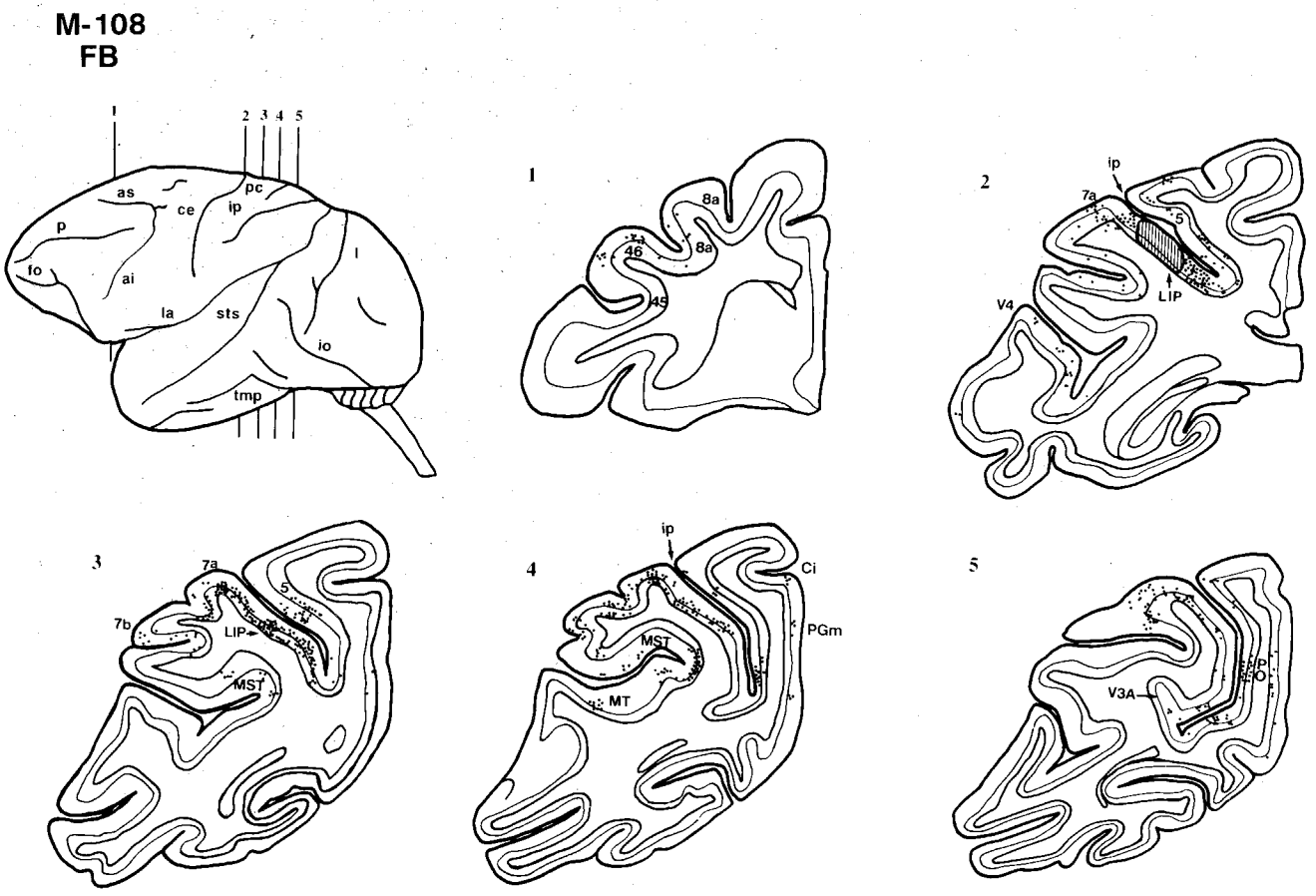

Fig. 13. Line drawings illustrating the injection site and pattern of retrogradely labeled cells in case M-108 from a fast blue (FB) injection in rostral LIP. The drawing at the upper right represents the levels from which coronal sections 1–5 were taken. From the FB injection illustrated in section 2, fluorescent retrogradely labeled cells were identified in areas 46 and 8a in the frontal lobe (section 1); dorsal V4, VIP, 5, and 7a (section 2); 7a, 7b, MST, and 5 (section 3); areas MT, MST, 7a, 7b, and PGm (section 4); and areas DP, V3A, and PO (section 5). The labeled cells in area 5 were most likely due to some leakage along the needle track as control injections in area 5 did not produce any retrogradely labeled cells in LIP (see Fig. 17). Note that areas 7b and PGm were not labeled from the anterograde injections in LIP (shown in Figs. 8, 11). Also, the retrogradely labeled cells in the frontal lobe are mostly in area 46 from this rostral injection in LIP similar to the autoradiographic injection in rostral LIP in case M-110 in Figure 8.

extremities) and/or touching the skin at or near a joint. The overall responses varied from simple (i.e., movement or touch localized to a single joint) to complex (i.e., more than one joint or movement involved). For example, many cells responded to rotation of one or two joints, usually in the same extremity. Some neurons, however, responded vigorously to extension in one extremity (e.g., forearm) and flexion of the same area in the opposite arm. Some neurons fired briskly to extension of a joint but were quiescent during flexion of the same joint. Most neurons (approximately 80%) were either restricted to the contralateral side or were both ipsilateral and contralateral. The remaining somatosensory responses were present only on the ipsilateral side.

TABLE 1. Response Properties of Area 5 Neurons

Modality	No. cells	% of total
Joint position	158	77.5
Touch	21	10.3
Joint position and touch	18	8.8
Visual	7	3.4
		n = 5
Total	204	*Macaca fascicularis*

Only seven cells responded positive to visual stimuli (slit of light on tangent screen while the monkey was in the dark), but the receptive fields of these cells were difficult to localize due to weak responses. In four cells, the receptive fields appeared "sickle" shaped extending across the horizontal meridian to include continuous parts of upper and lower contralateral visual fields at about 20–30° of eccentricity. However, the borders of these fields were not obvious.

Fluorescent retrograde tracer injections in area PEa

One of the two control injections in area PEa, the area on the medial bank of area 5, is illustrated in Figure 17. A DY injection in rostral area PEa in case M-100 resulted in retrogradely labeled cells in other areas known to have somatosensory functions such as areas 1, 2, SII, 7b (sections 1–3) and local connections to other areas in the superior parietal lobule (area PE; sections 2–4). In contrast to the many labeled cells in caudal visual area PO from LIP injections, many labeled cells were seen in visual area MDP (Colby et al., '88) from the rostral PEa injection. However, in a second case (M-108; not illustrated) involving a DY injection at a more caudal level in area PEa, retrogradely

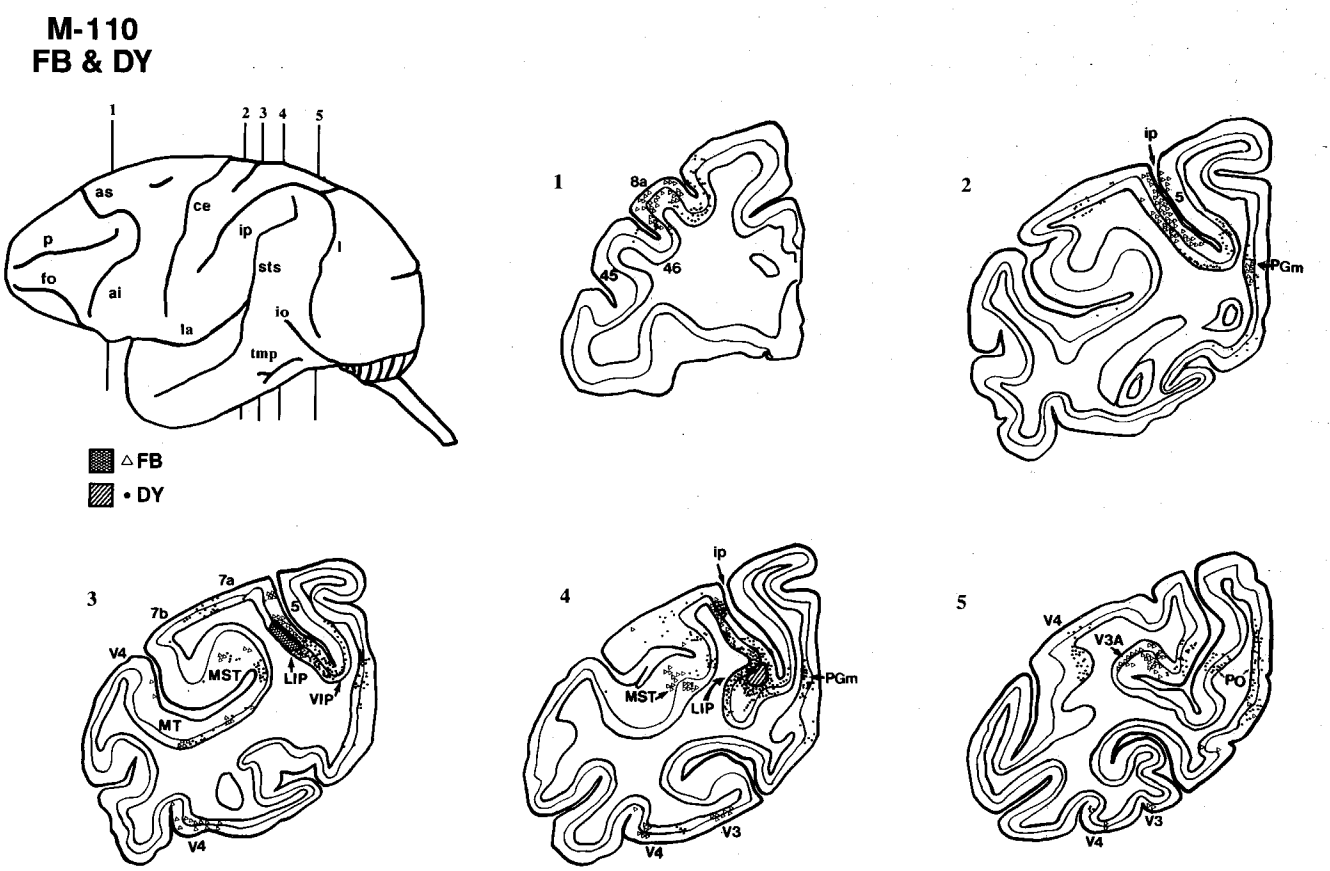

Fig. 14. Line drawings illustrating the injection sites and pattern of retrogradely labeled cells in case M-110 from a fast blue (FB) injection in rostral-intermediate LIP and a diamidino yellow (DY) injection in an intermediate level in LIP. The FB labeled cells are indicated by open triangles and the DY labeled cells are shown by solid dots in the five coronal sections. In section 1, a cluster of FB labeled cells is shown in lateral 8a, whereas an adjacent cluster of DY labeled cells is seen in the medial part of 8a. Area PGm is labeled from both injections (sections 2–4) although the FB cells predominated in rostral PGm (section 2), whereas the DY cells were mostly seen in caudal PGm (sections 3 and 4). This "clustering" of labeled cells (rather than an intermixing of DY and FB cells) was obvious in this case. Retrogradely labeled cells in dorsal V4, in 7b, and PO were only seen from the more caudal DY injection, whereas labeled cells in V3 and V3A (sections 4 and 5) were seen only from the rostral FB injection. Also, in ventral V4, the rostral FB injection labeled cells in rostral V4 whereas the more caudal DY injection labeled cells in caudal V4, suggesting a rostrocaudal topography of some afferents to parts of LIP.

labeled cells were seen in dorsal PO. Additional areas containing retrogradely labeled cells included areas TE2 and areas 1, 2, SII, and 7b. In contrast to LIP connections with the lateral pulvinar, area PEa injections labeled cells in the lateral posterior nucleus (LP; Fig. 17, section 2) and from the more caudal PEa injection (not illustrated) labeled cells were also apparent in the centrolateral nucleus (CL) and oral pulvinar. From the two PEa cases as well as from the LIP cases, the overall projection pattern from areas MDP and PO into area PEa and LIP is mapped in Figure 18. Area MDP projects more strongly to area PEa, while area PO sends a major projection to area LIP (Fig. 18). It is possible that the MDP projection to area PEa accounts for the few visual cells encountered in the area 5 mapping studies.

DISCUSSION

Findings reported in the present and previous studies from our laboratory strongly suggest that area LIP should be considered as a separate cortical area in the macaque inferior parietal lobule. First, the distinct cytoarchitectural and myeloarchitectural borders of LIP are in agreement with earlier observations (von Bonin and Bailey, '47; Seltzer and Pandya, '80; Pandya and Seltzer, '82; Siegel et al., '85). Second, the present study revealed a unique pattern of cortico-cortical and subcortical afferent and efferent connections of LIP. Third, single-unit recordings in the present study revealed a general order in contralateral receptive fields represented within rostrocaudal and dorsoventral parts of LIP which is very different from area 7a, which has larger bilateral receptive fields (Motter and Mountcastle, '81; Siegel et al., '85; Zipser and Andersen, '88; Andersen et al., '90a). Fourth, area LIP contains an abundance of neurons that are highly responsive to saccadic eye movements, and a large number of these cells are presaccadic (Gnadt et al., '86; Gnadt and Andersen, '88). In contrast, adjacent area 7a contains a smaller percentage of cells that are saccade-related and these neurons respond vigorously to postsaccadic events (Andersen and Gnadt, '89; Andersen et al., '90a).

Visual receptive field organization in area LIP

In the present study, many light sensitive cells with visual receptive fields were found in the lateral bank of the intraparietal sulcus. This is in agreement with our previous

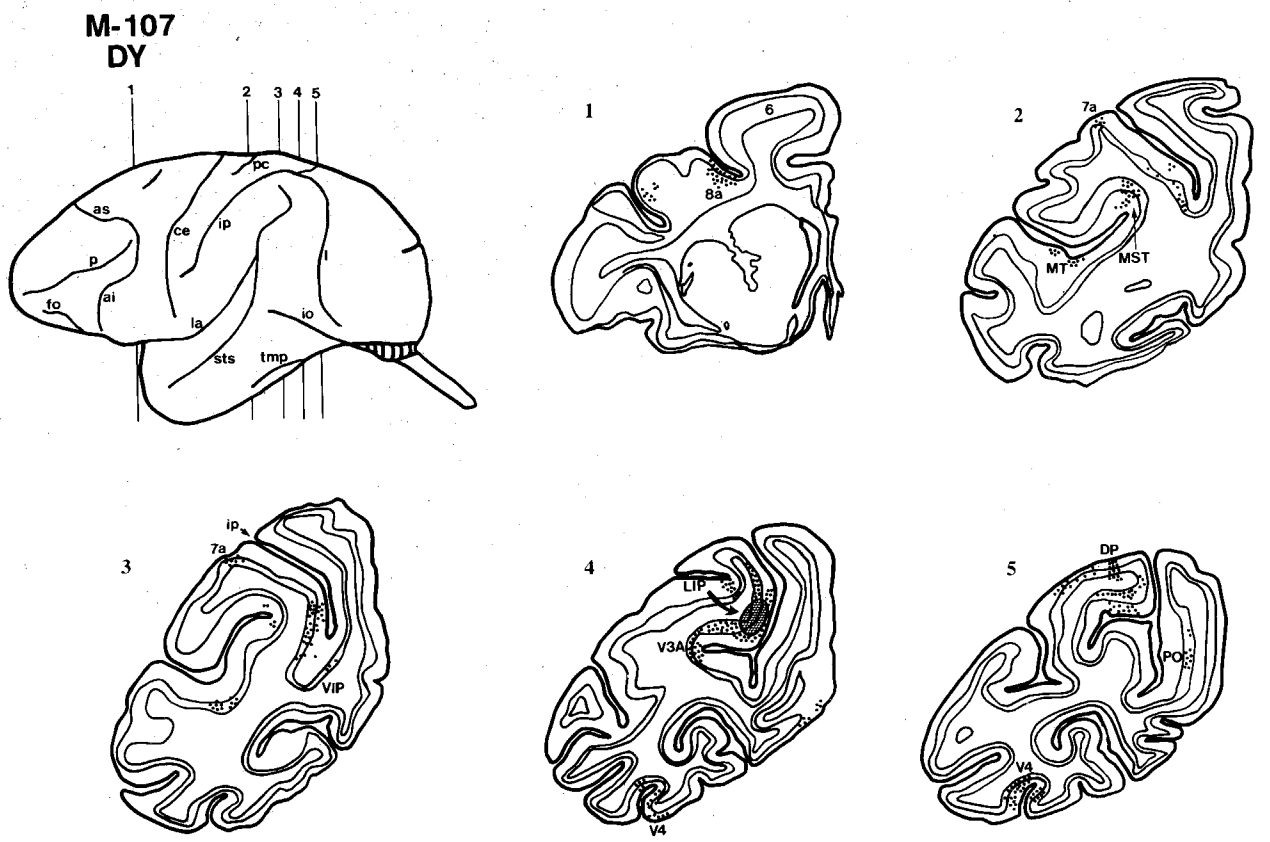

Fig. 15. Line drawings illustrating the injection site and pattern of retrogradely labeled cells in case M-107 from a DY injection in caudal LIP. A dense cluster of labeled cells is seen in area 8a in section 1 as well as a cluster at the 45/46 border. In sections 2 and 3, labeled cells are seen in areas 7a, MT, and MST with some cells also labeled in VIP. At the level of the injection site in section 4, dense label is seen in areas V3A and ventral V4. More caudally in section 5, the ventral V4 labeled cells persist and labeled cells were also present in dorsal V4, DP, and PO. Unlike the previous retrograde injections, no labeled cells were seen in areas V3, PGm, or 7b.

study in awake behaving rhesus monkeys in which neurons in area LIP were light sensitive and/or saccade-related (Gnadt et al., '86; Gnadt and Andersen, '88). In the present study, a systematic mapping of such visual receptive fields revealed a "rough" retinotopic organization that was highly organized (Fig. 5) but did include some systematic shifts in representation (Fig. 4). Within this course organization were areas of duplicate representation such that more than one part of LIP had the same representation of the upper or lower field. This is very similar to the receptive field organization found in areas V3A and V4 (Van Essen and Zeki, '78). In these areas, the contralateral visual field was represented in a highly complex organization revealing multiple representations of some parts of the visual field (Van Essen and Zeki, '78). Similar to area LIP, frontal eye field area 8a of Walker ('40), which receives a major projection from area LIP, also has small contralateral receptive fields (Suzuki and Azuma, '77). In contrast, large irregular bilateral receptive fields similar to those in area 7a have been reported for neurons in prefrontal cortical area 46 (Suzuki and Azuma, '77, '83; Funahashi et al., '85), which is a major projection field of area 7a (Siegel et al., '85; Andersen et al., '89). Area LIP also receives projections from area MST that contains large amorphous receptive fields in a mosaic type representation of the visual world (Desimone and Ungerleider, '86). In contrast, area LIP additionally receives projections from visual areas with retinotopically organized receptive fields such as area MT (Gattass and Gross, '81; Van Essen et al., '81; Desimone and Ungerleider, '86; Albright and Desimone, '87) and area PO, which has an emphasis on peripheral representation (Colby et al., '88). The receptive field size in LIP was variable with regard to eccentricity and the slope of the best fitting regression line was rather flat (b = 0.30). Interestingly, the slope of the regression line in LIP was almost identical to that reported for dorsal and ventral V3 and similar to those of dorsal and ventral V4 (Gattass et al., '88). However, the y-intercept for LIP was about 11°, whereas the y-intercept for V3 and V4 was about 1° or 2° (Gattass et al., '88). There also was much less variability in receptive field size with eccentricity in V3 and V4 than seen for LIP. These data suggest that LIP receptive fields are larger than either V3 or V4 in both central and peripheral representation and that there is a more course representation of the contralateral visual world in LIP than in V3 or V4. In contrast, the receptive fields in adjacent 7a are many-fold larger than those seen in LIP and many extend across the vertical meridian.

Relationship of area LIP with adjacent 7a and other extrastriate visual areas

While areas LIPv and 7a do have some common connections such as DP, MST, PO, PGm, 8a, and 46, many of their

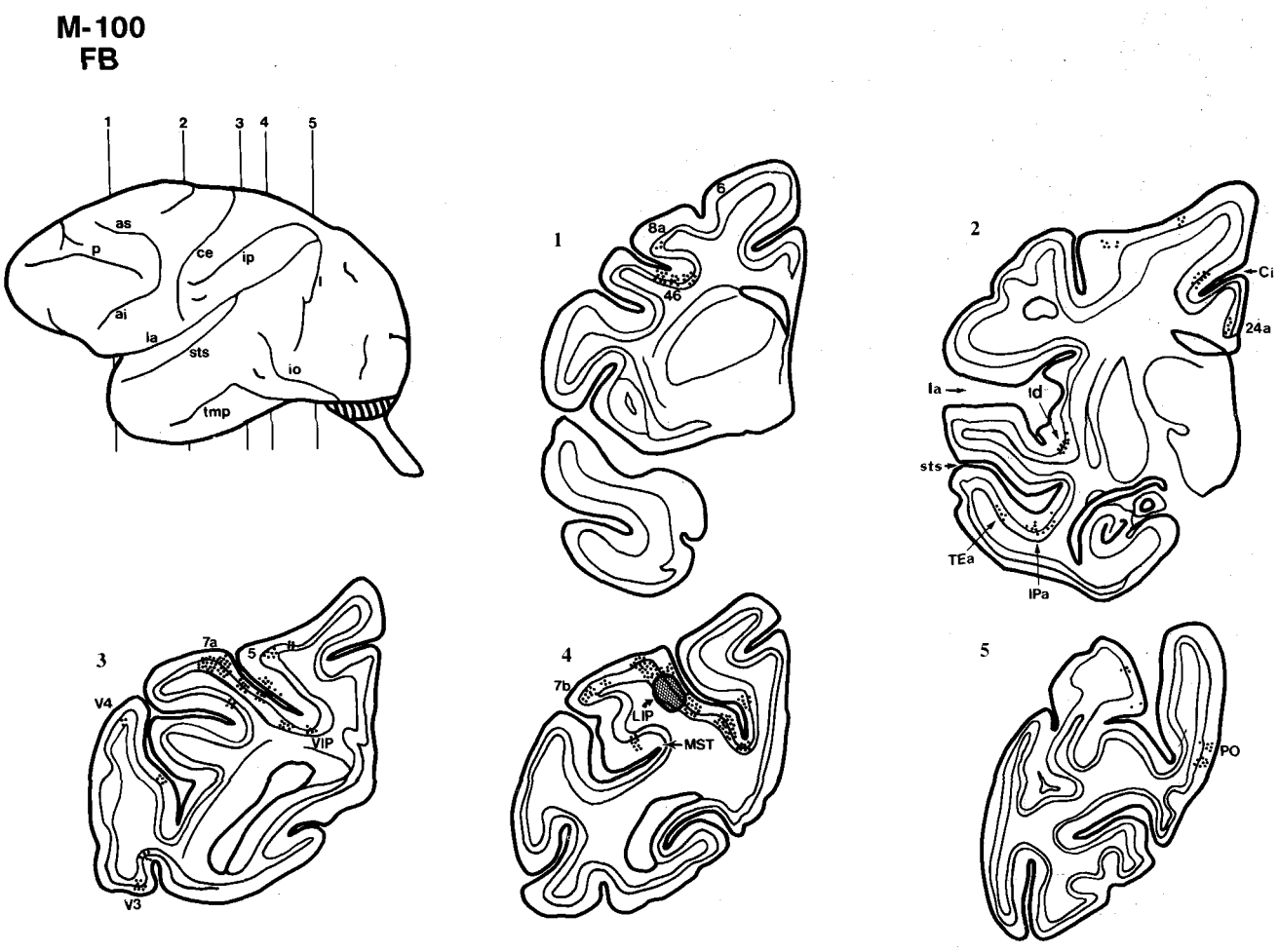

Fig. 16. Line drawing illustrating the injection site and pattern of retrogradely labeled cells in case M-100 from a FB injection in LIPd. Some common areas of label as seen from the other retrograde cases were apparent from this case. Similar areas of labeled cells included areas 8a and 46 (section 1); areas VIP, MST, 7a (sections 3 and 4), 7b, dorsal and ventral V3, and dorsal area V4 (section 3); and area PO (section 5). Retrogradely labeled cells were also seen in areas TEa and IPa, which were labeled only from the tritiated amino acid injection in case M-108 that was made high up in the lateral bank that included LIPd in the injection site. Additional areas of label were seen in the anterior cingulate gyrus in area 24a (section 2) and in the dysgranular insula (Id; section 2). In contrast to some of the other cases, there were not any retrogradely labeled cells in areas MT, ventral V4, or PGm in this case.

connections are different. For example, LIPv has connections with areas V3, V3A, V4, MT, Pul.l, Prt.a, and SC that are lacking with 7a (Asanuma et al., '85; Siegel et al., '85; Andersen et al., '90a). In contrast, area 7a has been shown to have strong connections with the presubiculum, area FST, the dorsal pretectal nucleus, medial pulvinar (Asanuma et al., '85), caudal cingulate area 23a, and area STP (Siegel et al., '85; Andersen et al., '90a) in the superior temporal gyrus. In addition, whereas only area MST projects to area 7a (Siegel et al., '85) results of the present study demonstrate that both areas MT and MST are connected to area LIP. The anterograde projection from LIPv to MST appears to be an intermediate type (Fig. 10; labeled terminals are spread across all laminae in area MST from amino acid injections in area LIP), whereas area MT sends a feedforward projection to area LIP and LIP sends a weak projection back to layer I in area MT (Fig. 9). Such a projection has been previously reported from MT to the lateral bank in area VIP as described by Ungerleider and Desimone ('86b), which overlaps with our area LIP. In that study (Ungerleider and Desimone, '86b), injections into the part of area MT with central field representation projected to the region of heavy myelination in the lateral bank, termed VIP* (i.e., corresponds to LIPv in the present study).

LIPv was found to send a "feedforward" projection to layers III and IV in 7a (Fig. 12) and, complementary amino acid injections in 7a (Andersen et al., '90a) yielded a "feedback" pattern of anterograde label strongest in layer I in LIP.

On the basis of these feedforward, feedback, and intermediate connections (Rockland and Pandya, '79; Maunsell and Van Essen, '83; Ungerleider and Desimone, '86b), Andersen et al. ('90a) recently placed area LIP in a high position in a hierarchy of visual connections in the primate brain. One such pathway, V1-MT-MST-7a, was constructed to explain the visual motion processing pathway (Maunsell and Van Essen, '83; Siegel et al., '85; Ungerleider and Desimone, '86a,b; Andersen, '87; Andersen et al., '90a). Since LIP has reciprocal "intermediate" connections with MST and receives input from MT and sends a "feedforward" projection

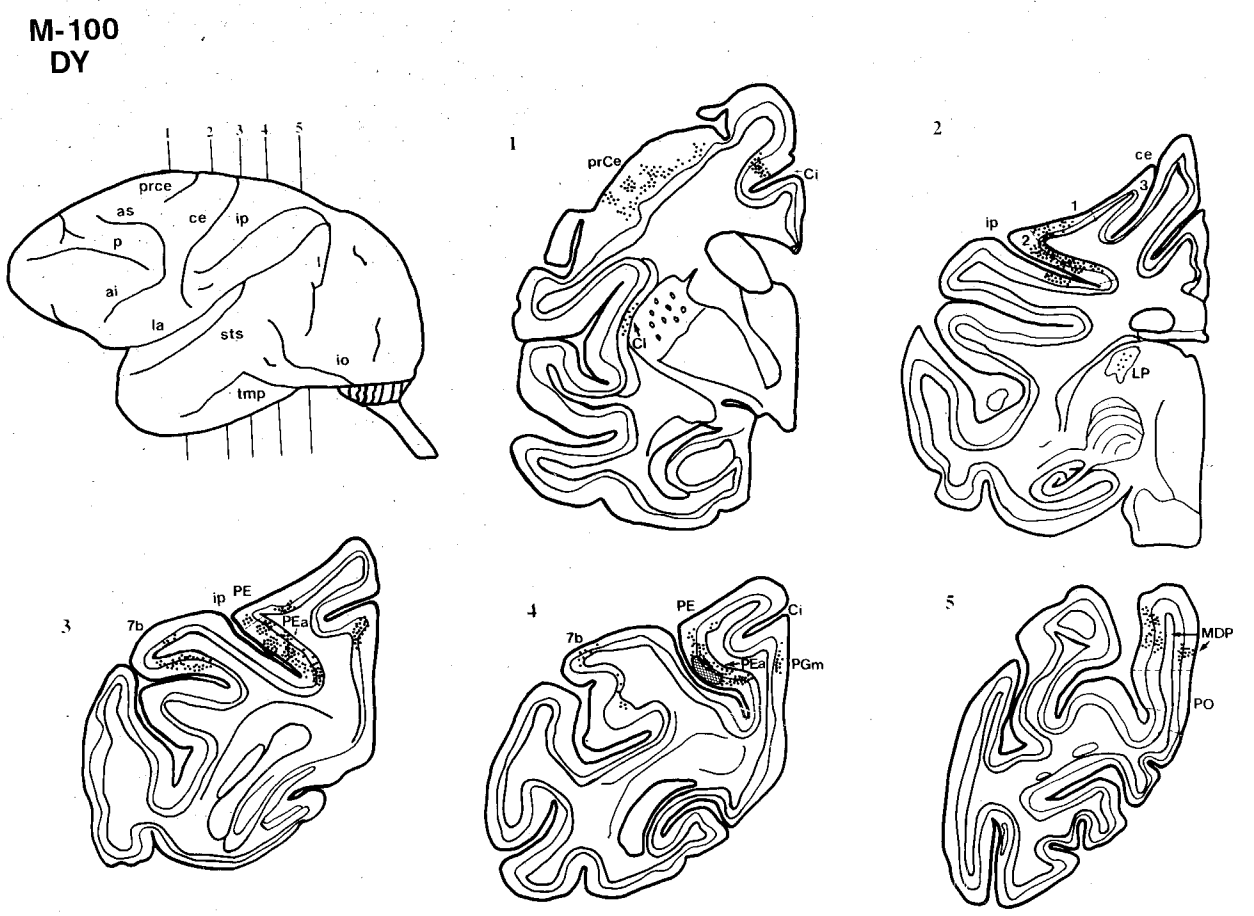

Fig. 17. Line drawings illustrating the injection site and pattern of retrogradely labeled cells in case M-100 from a DY injection in PEa of area 5 of the superior parietal lobule. The injection site in the medial bank is illustrated in section 4. There was no detectable leakage across the intraparietal sulcus into area LIP in this case. From this injection, retrogradely labeled cells were found along the precentral gyrus (prCe; section 1); in somatosensory areas 1, 2, and SII (section 2); in somatosensory areas 7b and PGm (sections 3–4); and in area MDP (section 5). Labeled cells were also found in the claustrum (Cl; section 1) and lateral posterior nucleus in the thalamus (LP; section 2). In contrast to the LIP injections (with the few exceptions above), no labeled cells were seen in the frontal, temporal or parietal extrastriate visual areas such as 7a, 8a, MT, MST, V3, V4, or DP. Some cells are seen in medial VIP (section 3) but may be due to diffusion from the site of injection.

to 7a, alternative or parallel processing pathways including V1-MT-LIP-7a or V1-MT-MST-LIP-7a may also exist in the macaque (Siegel et al., '85; Andersen et al., '90a). Recently, area VIP was reported to be a major recipient of MT projections (Maunsell and Van Essen, '83; Ungerleider and Desimone, '86b) and area VIP neurons' receptive fields and responsiveness are very similar to area MST neurons (Colby et al., '89) and thus may also play a role in motion processing. In addition, area VIP receives input from area V2 (Ungerleider and Desimone, '86a), while area LIP lacks such input.

There are additional data from the present investigation and from prior studies from our laboratory that strongly suggest that area LIPd should be included as part of LIP and not area 7a. For example, Gnadt and Andersen ('88) found many neurons responsive to saccadic eye movements in both the dorsal and ventral parts of LIP, but few saccade cells were seen in area 7a (Siegel et al., '85). In the present investigation, there was an orderly progression of visual receptive fields as the microelectrode passed through the dorsal and ventral parts of LIP, suggesting a continuous organization within LIP. For example, visual receptive fields mapped for LIPd neurons were primarily located in the central visual field with 15° of the fovea and as the microelectrode penetrated deeper along the lateral bank into LIPv, the mapped fields progressed to include more of the peripheral field (Fig. 5). In addition, the size of the receptive fields in dorsal LIP were similar to those mapped in ventral LIP and thus much smaller than those found for 7a. Similar to the connections of LIPv, the dorsal part of LIP receives afferents from areas 7a, 7b, 8a, 46, PO, V3, V4, and MST. However, LIPd also receives afferents from the superior temporal sulcus from visual area TEa (Baylis et al., '87) and multimodal area IPa (Pandya and Yeterian, '85; Baylis et al., '87; Pandya et al., '88) as well as the dysgranular insular cortex (Id), which receives strong somatosensory input from SII (Friedman et al., '86) and, from the rostral cingulate cortex (area 24a). It is interesting that the tritiated amino acid injection site in case M-108, which included part of LIPd, revealed anterograde projections to areas TEa, TEm, and IPa. These projections most likely arise from LIPd and not LIPv, where no such

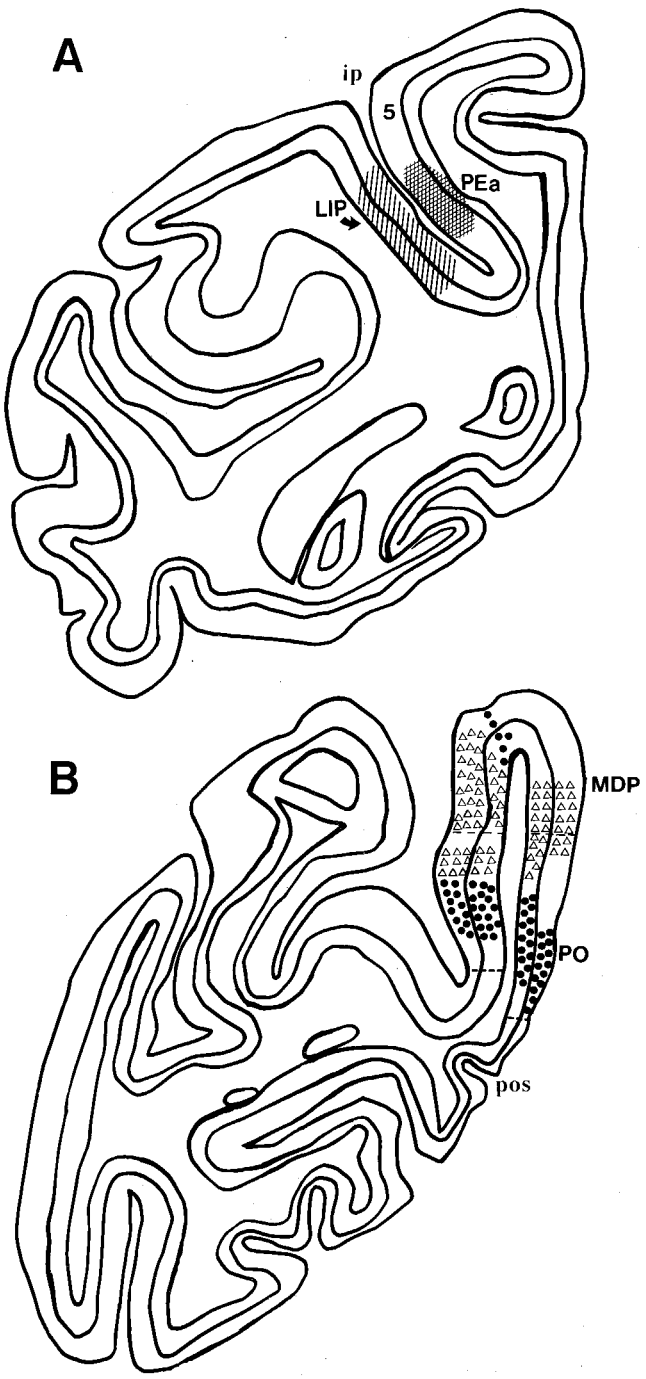

Fig. 18. Line drawings illustrating the projections from two visual areas at the border of the parietal and occipital lobes, areas MDP and PO to the medial (PEa) and lateral (LIP) banks along the intraparietal sulcus. These are composite drawings combining the locations of labeled cells from retrograde injections in the five cases. A topographic relationship of origin in the caudal lobule is present such that neurons in area MDP and in dorsal PO project to area PEa, whereas neurons in area PO and a few cells in the dorsolateral part of MDP project to LIP.

connections were seen in the other cases. Thus only dorsal LIP (and not LIPv or 7a) has connections with TEa, TEm, and IPa in temporal cortex and area 24a in anterior cingulate cortex, while only LIPv is reciprocally connected with MT. Area 7a also has connections to Id, the area in the ventral bank of the rostral STS, and the cingulate. One difficulty is the close proximity of LIPd to area 7a, and thus it is difficult to entirely restrict an injection to include only the dorsal part of LIP. Thus it is possible that some of these connections are due to tracer diffusing into 7a. On the other hand, LIPd should not be considered a part of 7a because injections of tracer that included primarily LIPv but also some of LIPd produced labelling indicative of LIP and, injections into LIPd also produced labelling indicative of LIP and only a weak and partial pattern indicative of 7a.

The majority of these data suggest that area LIP consists of a ventral and a dorsal part. However, it should also be considered that LIPd may have "unique" projections with visual and multimodal areas within the ventral bank of the superior temporal sulcus, Id and the cingulate. This implies that the two parts of LIP may play different roles in visuomotor integration and that given the proper physiological questions these possible differences may be revealed.

Visuomotor connections and properties of LIP neurons

It is now clear that there are strong connections between area LIP and eye-movement related areas in the macaque brain such as the frontal eye fields (Andersen et al., '85b; Siegel et al., '85; Goldman-Rakic, '88), the intermediate and deep layers of the superior colliculus (Asanuma et al., '85; Lynch et al., '85; Colby and Olsen, '85), and the anterior pretectal nuclei (Asanuma et al., '85). These LIP connections have been confirmed in the present study and have a functional correlate in that area LIP contains an abundance of cells highly responsive to saccadic eye movements (Shibutani et al., '84; Gnadt et al., '86; Gnadt and Andersen, '88). Deficits in such eye movements have been observed due to large bilateral parietal lesions in monkeys (Lynch, '80; Lynch and McLaren, '79, '82, '89) or via small ibotinic acid lesions in area LIP (Gnadt and Andersen, personal communication). For example, large bilateral parietal lesions in monkeys resulted in an increased mean saccade latency (Lynch and McLaren, '79, '82). These large lesions, however, included many visual areas in the posterior parietal cortex and thus failed to localize the deficit to any one particular area. In contrast, small ibotinic acid lesions restricted to area LIP in the rhesus monkey also produced deficits in eye movements. Following a lesion in the right hemisphere in area LIP, a monkey showed hypometric eye movements to the left, but only for eye movements to remembered target positions (Gnadt and Andersen, unpublished observations). The magnitude of these spatial distortions was dependent on the orbital positions from which the movements were made and was specific for the length and direction of the saccade. In another ibotinic acid lesion case, which was restricted to area LIP, the monkey made a series of two or three small saccades (approximately 5°), overshooting a remembered target 5° from the point of fixation instead of making a single smooth saccade to the target. This result suggests a possible disturbance in the feedback of information from the previous saccade or alternatively, a hyperactivity of remaining LIP neurons (Gnadt and Andersen, personal communication). It is interesting that

the deficits in the two ibotinic acid lesion cases only affected the memory-related saccades as a similar deficit has been recently reported to occur due to lesions in the dorsolateral prefrontal cortex (Goldman-Rakic, '87; Funahashi et al., '89).

Area LIP neurons in rhesus monkeys have also shown memory-linked motor planning activity which is the response representing the "intent" to make eye movements of specific amplitude and direction (Gnadt et al., '86; Gnadt and Andersen, '88; Andersen and Gnadt, '89). The activity of LIP neurons maintain a high firing rate during a delay period in which the monkey is withholding an eye movement until a fixation spot is extinguished. Once the animal has made the eye movement, the cells' activities return to baseline. Special double saccade experiments showed that the cells were coding in motor coordinates and therefore the activity represents the intended movement stored in short-term memory, rather than the retinal or spatial location of the stimulus. This intended movement activity, found in cells in LIP, is very similar to findings of Mays and Sparks ('80) from recordings made in the superior colliculus. These investigators termed such units "quasi-visual cells"; these cells were located in the intermediate layers of the superior colliculus which is a target of LIP projections (Asanuma et al., '85; Lynch et al., '85; Colby and Olsen, '85). Similar memory-related activity has also been shown for neurons in the frontal eye fields (Bruce and Goldberg, '85) and for neurons near the principal sulcus in prefrontal cortex (Funahashi et al., '89), although these studies did not determine whether the cells were coding in sensory or motor coordinates.

An important discovery in the present investigation was that the area LIP reciprocal connections with the dorsolateral frontal lobe are topographically organized such that the rostral-intermediate parts of LIPv were connected to lateral 8a and medial 46 whereas the caudal part of LIPv was connected to medial 8a (Fig. 14). Also, LIPd has more extensive connections with area 46 and only sparse connections with 8a. There is physiological evidence that saccade amplitude and direction is topographically organized in the frontal eye fields (Bruce et al., '85). The largest saccades (extending to the periphery) were elicited from the most dorsolateral part of area 8a, while the smallest saccades were elicited from the ventrolateral portion (Robinson and Fuchs, '69; Bruce et al., '85). Similar studies need to be performed in area LIP to determine whether saccade amplitude and direction in cells in different parts of LIP correlate with similar saccades elicited in the parts of the frontal eye fields that are topographically connected with LIP.

Although areas LIP and 7a are reciprocally connected, it is not known how or if neurons in the two areas influence the functional roles these areas may have in visuospatial processing. Recent studies have shown that visual responses in area 7a are dependent on eye position (Andersen and Mountcastle, '83; Andersen et al., '85a). Although the receptive fields remain retinotopic, the magnitude of the visual response is modulated by eye position. Andersen et al. ('85a) proposed that this interaction of retinal and eye position signals may be part of a neural mechanism for encoding the location of visual stimuli in head-centered coordinates. A recent neural network model trained to localize position in head-centered space produced interaction of retinal and eye position signals like those recorded in area 7a (Zipser and Andersen, '88). Recently, it has been shown that the visual, intended movement and saccade responses of area LIP neurons are also modulated by eye position in a similar fashion to area 7a cells (Andersen et al., '90b). The programming of saccades requires a coordinate transformation from a visual input, which is coded in head-centered coordinates (Andersen and Goodman, '89). The modulation of area LIP responses by eye position may indicate that this area plays a role in this coordinate transformation (Andersen and Goodman, '89). Certainly, connections with other cortical and subcortical structures that integrate visuomotor information are most likely essential elements to this ability to perform these coordinate transformations.

Somatosensory connections of area LIP

A major somatosensory input has been reported into the area of cortex just rostral to LIP, in rostral area POa of Seltzer and Pandya ('80; Pandya and Seltzer, '82). In the present study, the more caudal part of POa that included area LIP had more limited connections with somatosensory areas. Area LIP does receive input from area 7b (PF), which is in agreement with the findings of Seltzer and Pandya ('80) and Pandya and Seltzer ('82). Andersen et al. ('90a) reported that area 7b receives input from area 5. Some retrogradely labeled cells were seen in area PEa from the dye injections in LIP and anterograde label was seen in area PEa following tritiated amino injections in LIP, which agrees with previous findings (Pandya and Seltzer, '82; Neal et al., '86). However, no retrogradely labeled cells were seen in LIP following control injections limited to sulcal area 5 (PEa). Therefore, the results from this study suggest that area LIP is not connected to PEa and that the label in PEa after LIP injections is due to leakage of tracer up the electrode track through area PEa.

There was also label in the dysgranular insula (Id) following LIPd injections. This part of the insula receives its major input from secondary somatosensory association cortex (SII) and is known to project to the amygdala, perirhinal cortex (Friedman et al., '86), and to posterior parahippocampal gyrus (Blatt et al., '89). Interestingly, LIPd projects to the same part of the lateral posterior parahippocampal area (area TF) that receives a strong projection from the dysgranular insula (Blatt et al., '89).

Response properties of area 5 neurons and visual inputs to area PEa

Single-unit recordings in 204 neurons in area 5 revealed that 96.6% of these neurons were responsive to mechanical stimulation of one or more joints (i.e., usually ipsilateral and/or contralateral flexion or extension of the arm or leg) or touching the skin at or near one of these joints (Table 1). These findings are in agreement with previous mapping studies in area 5 (Duffy and Burchfield, '71; Sakata et al., '73; Sakata, '75; Mountcastle et al., '75; MacKay et al., '78).

The remaining tested neurons in area 5 in the present study (3.4%) were responsive to visual stimuli. The receptive fields of these cells were vague but they appear to include continuous parts of both the upper and lower contralateral visual fields. This rare occurrence of visual cells in area 5 agrees with a previous study by Mountcastle et al. ('75), who found six visually responsive neurons out of 977 they studied (0.6%). The anatomical experiments of the present study demonstrated possible visual inputs to the

sulcal part of area 5 (PEa) from area MDP and ventral PO. The complementary projection from area 5 to PO and MDP was demonstrated by Colby et al. ('88) from fluorescent tracer injections in PO or MDP with retrogradely labeled cells found in the medial intraparietal area (MIP), which is equivalent to PEa. The possible visual inputs to area PEa from MDP and PO, as demonstrated in the present study, originate from populations of neurons separate than those that project from these same areas to LIP (Fig. 18). Mapping studies in area PO by Covey et al. ('82) and Colby et al. ('88) demonstrated that neurons in PO emphasize peripheral field representation. This presumed visual input may be important in such tasks as reaching (arm projection and manipulation) as such neurons have been identified in area 5 (9% of sampled neurons) by Mountcastle et al. ('75) as well as in area 7b (30% of sampled neurons) by Hyvarinen and Poranen ('74) in posterior parietal cortex.

ACKNOWLEDGMENTS

The authors would like to thank Drs. Jim Gnadt and Ralph Siegel for their invaluable assistance and Karen Sutter for technical assistance. Special thanks to Dr. Colin Bernstein for his ophthalmic assistance with the monkeys. This work was supported by NIH grants EY05522 and EY07492, a McKnight Foundation Scholars award to R.A.A., the Sloan Foundation, and the Clayton Foundation.

LITERATURE CITED

Albright, T.D., and R. Desimone (1987) Local precision of visuotopic organization in the middle temporal area (MT) of the macaque. Exp. Brain Res. *65:*582–592.

Allman, J.M., and J.H. Kaas (1971) A representation of the visual field in the caudal third of the middle temporal gyrus of the owl monkey (Aotus trivirgatus). Brain Res. *31:*85–105.

Andersen, R.A. (1987) Inferior parietal lobule function in spatial perception and visuomotor integration. In V.B. Mountcastle, F. Plum, and S.R. Geiger (eds): Handbook of Physiology: The Nervous System, Vol. 5 (1). Bethesda, MD: American Physiological Society, pp. 483–518.

Andersen, R.A., and V.B. Mountcastle (1983) The influence of the angle of gaze upon the excitability of the light-sensitive neurons of the posterior parietal cortex. J. Neurosci. *3(3):*532–548.

Andersen, R.A., and J.W. Gnadt (1989) Posterior parietal cortex. In R. Wurtz and M.E. Goldberg (eds): The Neurobiology of Saccadic Eye Movements. Amsterdam: Elsevier, pp. 315–335.

Andersen, R.A., and S.J. Goodman (1989) Microstimulation of a neural network model that computes coordinate transformations for visually guided saccades. Soc. Neurosci. Abstr. *15:*1204.

Andersen, R.A., G.K. Essick, and R.M. Siegel (1985a) Encoding of spatial location by posterior parietal neurons. Science *230:*456–458.

Andersen, R.A., C. Asanuma, and W.M. Cowan (1985b) Callosal and prefrontal associational projecting cell populations in area 7a of the macaque monkey: A study using retrogradely transported fluorescent dyes. J. Comp. Neurol. *232:*443–455.

Andersen, R.A., G.K. Essick, and R.M. Siegel (1987) Neurons of area 7 activated by both visual stimuli and oculomotor behavior. Exp. Brain Res. *67:*316–322.

Andersen, R.A., C. Asanuma, G. Essick, and R.M. Siegel (1990a) Corticocortical connections of anatomically and physiologically defined subdivisions within the inferior parietal lobule. J. Comp. Neurol. *296:*65–113.

Andersen, R.A., R.M. Bracewell, S. Barash, J.W. Gnadt, and L. Fogassi (1990b) Eye position effects on visual memory and saccade related activity in areas LIP and 7a of macaque. J. Neurosci. *10:*1176–1196.

Asanuma, C., R.A. Andersen, and W.M. Cowan (1985) The thalamic relations of the caudal inferior parietal lobule and the lateral prefrontal cortex in monkeys: Divergent cortical projections from cell clusters in the medial pulvinar nucleus. J. Comp. Neurol. *241:*357–381.

Barash, S., R.M. Bracewell, L. Fogassi, and R.A. Andersen (1989) Interactions of visual and motor-planning activities in the lateral intraparietal area. Soc. Neurosci. Abstr. *15:*1203.

Barbas, H., and M.-M. Mesulam (1981) Organization of afferent input to subdivisions of area 8 in the rhesus monkey. J. Comp. Neurol. *200:*407–431.

Baylis, G.C., E.T. Rolls, and C.M. Leonard (1987) Functional subdivisions of the temporal lobe neocortex. J. Neurosci. *7(2):*330–342.

Blatt, G.J., G.R. Stoner, and R.A. Andersen (1987) The lateral intraparietal area (LIP) in the macaque: Associational connections and visual receptive field organization. Soc. Neurosci. Abstr. *13:*627.

Blatt, G.J., D.L. Rosene, and D.N. Pandya (1989) Cortical afferents to the posterior parahippocampal gyrus of the rhesus monkey. I. Input from limbic, multimodal and unimodal areas in temporal, insular, parietal and occipital cortices. Soc. Neurosci. Abstr. *15:*342.

Bruce, C.J., and M.E. Goldberg (1985) Primate frontal eye fields. I. Single neurons discharging before saccades. J. Neurophysiol. *53:*603–635.

Bruce, C.J., M.E. Goldberg, M.C. Bushnell, and G.B. Stanton (1985) Primate frontal eye fields. II. Physiological and anatomical correlates of electrically evoked eye movements. J. Neurophysiol. *54:*714–734.

Colby, C.L., and C.R. Olsen (1985) Visual topography of cortical projections to monkey superior colliculus. Soc. Neurosci. Abstr. *11:*1244.

Colby, C.L., R. Gattass, C.R. Olsen, and C.G. Gross (1988) Topographical organization of cortical afferents to extrastriate visual area PO in the macaque: A dual tracer study. J. Comp. Neurol. *269:*392–413.

Colby, C.L., J.-R. Duhamel, and M.E. Goldberg (1989) Visual response properties and attentional modulation of neurons in the ventral intraparietal area in the alert monkey. Soc. Neurosci. Abstr. *15:*162.

Covey, E., R. Gattass, and C.G. Gross (1982) A new visual area in the parieto-occipital sulcus of the macaque. Soc. Neurosci. Abstr. *8(2):*681.

Cowan, W.M., D.I. Gottleib, A.E. Hendrickson, J.L. Price, and T.A. Woolsey (1972) The autoradiographic demonstration of axonal connections in the central nervous system. Brain Res. *37:*21–51.

Desimone, R., and L.G. Ungerleider (1986) Multiple visual areas in the caudal superior temporal sulcus of the macaque. J. Comp. Neurol. *248(2):*164–189.

Duffy, F.H., and J.L. Burchfield (1971) Somatosensory system: Organizational hierarchy from single units in monkey area 5. Science *172:*273–275.

Duhamel, J.-R., C.L. Colby, and M.E. Goldberg (1989) Congruent visual and somatosensory response properties of neurons in the ventral intraparietal area in the alert monkey. Soc. Neurosci. Abstr. *15:*162.

Friedman, D.P., E.A. Murray, J.B. O'Neill, and M. Mishkin (1986) Cortical connections of the somatosensory fields of the lateral sulcus of macaques: Evidence for a corticolimbic pathway for touch. J. Comp. Neurol. *252:*323–347.

Funahashi, S., C.J. Bruce, and P.S. Goldman-Rakic (1985) Visual properties of prefrontal neurons. Soc. Neurosci. Abstr. *11:*525.

Funahashi, S., C.J. Bruce, and P.S. Goldman-Rakic (1989) Mnemonic coding of visual space in the monkey's dorsolateral prefrontal cortex. J. Neurophysiol. *61:*331–349.

Gallyas, F. (1979) Silver staining of myelin by means of physical development. Neurol. Res. *1:*203–209.

Gattass, R., and C.G. Gross (1981) Visual topography of the striate projection zone in the posterior superior temporal sulcus (MT) of the macaque. J. Neurophysiol. *46:*521–538.

Gattass, R., A.P.B. Sousa, and C.G. Gross (1988) Visuotopic organization and extent of V3 and V4 of the macaque. J. Neurosci. *8(6):*1831–1845.

Gnadt, J.W., and R.A. Andersen (1988) Memory related motor planning activity in posterior parietal cortex of macaque. Exp. Brain Res. *70:*216–220.

Gnadt, J.W., R.A. Andersen, and G.J. Blatt (1986) Spatial, memory and motor planning properties of saccade-related activity in the lateral intraparietal area (LIP) of macaque. Soc. Neurosci. Abstr. *12:*454.

Goldman-Rakic, P.S. (1987) Circuitry of primate prefrontal cortex and regulation of behavior by representational memory. In Mountcastle, F. Plum, and S.R. Geiger (eds): Handbook of Physiology: The Nervous System, vol. 5(1). Bethesda, MD: American Physiological Society, pp. 373–418.

Goldman-Rakic, P.S. (1988) Topography of cognition: Parallel distributed networks in primate association cortex. Annu. Rev. Neurosci. *11:*137–156.

Hedreen, J.C., and T.C.T. Yin (1981) Homotopic and heterotopic callosal afferents of caudal inferior parietal lobule in Macaca mulatta. J. Comp. Neurol. *197:*605–621.

Hyvarinen, J. (1982) The parietal cortex of monkey and man. In H.B. Barlow, H. Bullock, E. Florey, O.-J. Grusser and A. Peters (eds): Studies of Brain Function, vol. 8. Berlin: Springer-Verlag, pp. 1–202.

Hyvarinen, J., and A. Poranen (1974) Function of the parietal associative area 7 as revealed from cellular discharges in alert monkeys. Brain *97:*673–692.

Keizer, K., H.G.J.M. Kuypers, A.M. Huisman, and O. Denn (1983) Diamidino yellow dihydrochloride (DY 2HCL): A new fluorescent retrograde neuronal tracer which migrates only very slowly out of the cell. Exp. Brain Res. *51:*179–191.

Kuypers, H.G.J.M., M. Bentiviglio, C.E. Entomes-Bernevoets, and A.T. Bharos (1980) Double retrograde labeling through divergent axon collaterals using two fluorescent tracers with the same excitation wavelength which label two different features of the cell. Exp. Brain Res. *40:*383–392.

Lynch, J.C. (1980) The functional organization of posterior parietal association cortex. Behav. Brain Sci. *3:*485–499.

Lynch, J.C., and J.W. McLaren (1979) Effects of lesions of parieto-occipital association cortex upon performance of oculomotor and attention tasks in monkeys. Soc. Neurosci. Abstr. *5:*794.

Lynch, J.C., and J.W. McLaren (1982) The contribution of parieto-occipital association cortex to the control of slow eye movements. In G. Lennerstrand and D.S. Zee (eds): Functional Basis of Ocular Motility Disorders, Oxford: Pergamon Press, pp. 501–515.

Lynch, J.C., A.M. Graybiel, and L.J. Lobeck (1985) The differential projection of two cytoarchitectonic subregions of the inferior parietal lobule of macaque upon the deep layers of the superior colliculus. J. Comp. Neurol. *235:*241–254.

MacKay, W.A., M.C. Kwan, J.T. Murphy, and Y.C. Wong (1978) Responses to active and passive wrist rotation in area 5 of awake monkeys. Neurosci. Lett. *10:*235–239.

Maunsell, J.H.R., and D.C. Van Essen (1983) The connections of the middle temporal visual area (MT) and their relationship to a cortical hierarchy in the macaque monkey. J. Neurosci. *3:*2563–2586.

Mays, L.E., and D.L. Sparks (1980) Dissociation of visual and saccade-related responses in superior colliculus neurons. J. Neurophysiol. *43:*207–232.

Mesulam, M.-M., G.W. Van Hoesen, D.N. Pandya, and N. Geschwind (1977) Limbic and sensory connections of the inferior parietal lobule (area PG) in the rhesus monkey: A study with a new method for horseradish peroxidase histochemistry. Brain Res. *136:*393–414.

Motter, B.C., and V.B. Mountcastle (1981) The functional properties of the light-sensitive neurons of the posterior parietal cortex studied in waking monkeys: Foveal sparing and opponent vector organization. J. Neurosci. *1:*3–26.

Mountcastle, V.B., J.C. Lynch, A. Georgopoulos, H. Sakata, and C. Acuna (1975) Posterior parietal association cortex of the monkey: Command functions for operations within extrapersonal space. J. Neurophysiol. *38:*871–907.

Neal, J.W., R.C.A. Pearson, and T.P.S. Powell (1986) The organization of the corticocortical projection of area 5 upon area 7 in the parietal lobe of the monkey. Brain Res. *381:*164–167.

Neal, J.W., R.C.A. Pearson, and T.P.S. Powell (1988a) The cortico-cortical connections within the parieto-temporal lobe of area PG, 7a, in the monkey. Brain Res. *438:*343–350.

Neal, J.W., R.C.A. Pearson, and T.P.S. Powell (1988b) The organization of the cortico-cortical connections between the walls of the lower part of the superior temporal sulcus and the inferior parietal lobule in the monkey. Brain Res. *438:*351–356.

Pandya, D.N., and B. Seltzer (1982) Intrinsic connections and architectonics of posterior parietal cortex in the rhesus monkey. J. Comp. Neurol. *204:*196–210.

Pandya, D.N., and E.H. Yeterian (1985) Architecture and connections of cortical association areas. In A. Peters and E.G. Jones (eds): Cerebral Cortex, Vol. 4. New York: Plenum Press, pp. 3–61.

Pandya, D.N., B. Seltzer, and H. Barbas (1988) Input-output organization of the primate cerebral cortex. In H.D. Steklis and J. Erwin (eds): Comparative Primate Biology, Volume 4: Neurosciences. New York: Alan R. Liss, Inc., pp. 39–80.

Robinson, D.A., and A.F. Fuchs (1969) Eye movements evoked by stimulation of frontal eye fields. J. Neurophysiol. *32:*637–648.

Rockland, K.S., and D.N. Pandya (1979) Laminar origins and terminations of cortical connections of the occipital lobe in the rhesus monkey. Brain Res. *179:*3–20.

Sakata, H. (1975) Somatic sensory responses of neurons in the parietal association area (area 5) in monkeys. In H.H. Kornhuber (ed): The Somatosensory System. Stuttgart: Thieme, pp. 250–261.

Sakata, H., A. Takaoka, A. Kawarasaki, and H. Shibutani (1973) Somatosensory properties of neurons in superior parietal cortex (area 5) of the rhesus monkey. Brain Res. *64:*85–102.

Seal, J., C. Gross, and B. Bioulac (1982) Activity of neurons in area 5 during a simple arm movement in monkeys before and after deafferentation of the trained limb. Brain Res. *250:*229–243.

Seal, J., C. Gross, D. Doudet, and B. Bioulac (1983) Instruction-related changes of neuronal activity in area 5 during a simple forearm movement in the monkey. Neurosci. Lett. *36:*145–150.

Seltzer, B., and G.W. Van Hoesen (1979) A direct inferior parietal lobule projection to the presubiculum in the rhesus monkey. Brain Res. *179:*157–162.

Seltzer, B., and D.N. Pandya (1980) Converging visual and somatic sensory cortical input to the intraparietal sulcus of the rhesus monkey. Brain Res. *192:*339–351.

Seltzer, B., and D.N. Pandya (1984) Further observations on parieto-temporal connections in the rhesus monkey. Exp. Brain Res. *55:*301–312.

Shibutani, H., H. Sakata, and J. Hyvarinen (1984) Saccade and blinking evoked by microstimulation of the posterior parietal association cortex of the monkey. Exp. Brain Res. *55:*1–8.

Siegel, R.M., R.A. Andersen, G.K. Essick, and C. Asanuma (1985) The functional and anatomical subdivision of the inferior parietal lobule. Soc. Neurosci. Abstr. *11:*1012.

Sokal, R.R., and F.J. Rohlf (1973) Introduction to Biostatistics. San Francisco: W.H. Freeman, Co., pp. 134–161, 225–259.

Stoner, G.R., G.J. Blatt, and R.A. Andersen (1987a) Anatomical connections and receptive field organization of the lateral intraparietal area (LIP) in the macaque. The Second World Congress of Neuroscience (IBRO). Neuroscience [Suppl.] *22:*S733.

Stoner, G.R., G.J. Blatt, and R.A. Andersen (1987b) Retrograde connections of the sulcal region of the superior parietal lobule (area 5) in the macaque. Soc. Neurosci. Abstr. *13:*626.

Suzuki, H., and M. Azuma (1977) Prefrontal neuronal activity during gazing at a light spot in the monkey. Brain Res. *126:*497–508.

Suzuki, H., and M. Azuma (1983) Topographic studies on visual neurons in the dorsolateral prefrontal cortex of the monkey. Exp. Brain Res. *53:*47–58.

Ungerleider, L.G., and R. Desimone (1986a) Projections to the superior temporal sulcus from the central and peripheral field representations of V1 and V2. J. Comp. Neurol. *248(2):*147–163.

Ungerleider, L.G., and R. Desimone (1986b) Cortical connections of visual area MT in the macaque. J. Comp. Neurol. *248(2):*190–222.

Van Essen, D.C., and Zeki, S.M. (1978) The topographic organization of rhesus monkey prestriate cortex. J. Physiol. (Lond.) *277:*193–226.

Van Essen, D.C., J.H.R. Maunsell, and J.L. Bixby (1981) The middle temporal visual area in the macaque: Myeloarchitecture, connections, functional properties and topographic organization. J. Comp. Neurol. *199:*293–326.

Vogt, C., and O. Vogt (1919) Allgemeine Ergebnisse unserer Hirnforschung. J. Psychol. Neurol. *25:*279–462.

von Bonin, G., and P. Bailey (1947) The Neocortex of Macaca Mulatta, Urbana: University of Illinois Press.

Walker, A.E. (1940) A cytoarchitectural study of the pre-frontal area of the macaque monkey. J. Comp. Neurol. *73:*59–86.

Yeterian, E.H., and D.N. Pandya (1985) Corticothalamic connections of the posterior parietal cortex in the rhesus monkey. J. Comp. Neurol. *237:*408–426.

Zipser, D., and R.A. Andersen (1988) A back-propagation programmed network that simulates response properties of a subset of posterior parietal neurons. Nature *331:*679–684.